Surface photometry of low surface brightness galaxies

de Blok, WJG; van der Hulst, J.M.; Bothun, GD

Published in:
Monthly Notices of the Royal Astronomical Society

DOI:
10.1093/mnras/274.1.235

Publication date:
1995

Mon. Not. R. Astron. Soc. **274**, 235–255 (1995)

Surface photometry of low surface brightness galaxies

W.J.G. de Blok,[1] J.M. van der Hulst[1] and G.D. Bothun[2]
[1]*Kapteyn Astronomical Institute, PO Box 800, 9700 AV Groningen, The Netherlands*
[2]*Department of Physics, University of Oregon, Eugene, Oregon 97403, USA*

Accepted 1994 November 30. Received 1994 November 4; in original form 1994 August 2

ABSTRACT
Low surface brightness (LSB) galaxies are galaxies dominated by an exponential disc whose central surface brightness is much fainter than the value of $\mu_B(0) = 21.65 \pm 0.30$ mag arcsec^{-2} found by Freeman. In this paper we present broadband photometry of a sample of 21 late-type LSB galaxies. The median central surface brightness of the sample is $\mu_B(0) = 23.2$ mag arcsec^{-2} and the median scale length is 3.2 kpc, showing that LSB galaxies are normal-sized galaxies. We find colours that are comparable to or bluer than those of the more widely studied 'normal' high surface brightness (HSB) galaxies. LSB galaxies are therefore not faded discs that have no current star formation. The colours cannot on the other hand be ascribed entirely to metallicity effects, but we can explain them by assuming a sporadic star formation rate scenario. LSB galaxies hence appear to be unevolved and quiescent objects, which give us an insight into the evolution of galaxies in an unperturbed environment.

Key words: galaxies: evolution – galaxies: fundamental parameters – galaxies: photometry – galaxies: spiral – galaxies: stellar content.

1 INTRODUCTION

1.1 Freeman's Law and selection effects

One of the most well-known early results derived from surface photometry of spiral galaxies is Freeman's Law (Freeman 1970). Freeman analysed the photometry of disc galaxies available at that time and found the remarkable result that the central surface brightnesses of 28 of the 36 discs studied fell within the range of $\mu_B(0) = 21.65 \pm 0.30$ mag arcsec^{-2}. This result has been widely discussed. Some showed that the effect might be real (van der Kruit 1987; Bosma & Freeman 1993), while others suggested that the 'law' is a selection effect (Disney 1976; Allen & Shu 1979; Disney & Phillips 1983; Davies 1990), or results from extinction (Valentijn 1990; Huizinga 1994) or a combination of both. It has now become clear that disc galaxies exhibit a large range in central surface brightness, contrary to Freeman's Law (de Jong & van der Kruit 1994).

The brightness of the night sky results in a strong bias against objects with central surface brightnesses much fainter than the Freeman value. These objects are less likely to meet the selection criteria of the major galaxy catalogues and will be under-represented.

Recent surveys (e.g. Schombert & Bothun 1988; Schombert et al. 1992 [hereafter SBSM]) have shown the presence of many field galaxies with peak surface brightnesses much fainter than the surface brightness of the night sky. Selection effects are thus determining our view of the Universe. However, studies of these low surface brightness (LSB) galaxies have begun to tell us more about this visually less prominent part of the total galaxy population.

1.2 Low surface brightness galaxies

We have begun a systematic programme to use multicolour and Hα surface photometry, spectrophotometry and H I observations of a sample of $\sim$ 20 LSB galaxies, to determine the distributions of light, colour, H II-, H I-, and mass surface density, and elemental abundances, with the ultimate goal to unravel the star formation history of LSB galaxies. In this paper we present structural parameters and colours of our sample of LSB galaxies as derived from optical multicolour broad-band data.

We define a LSB galaxy to be a galaxy which is dominated by an exponential disc with a face-on central disc surface brightness which is more than one magnitude fainter than the Freeman value of $\mu_B(0) = 21.65$ mag arcsec^{-2}. This group of objects is relatively poorly studied, and under-represented in many catalogues.

A typical LSB galaxy resembles a normal late-type spiral, usually with a few ill-defined spiral arms. It contains only a few H II regions, which do not trace the spiral arms very well and are usually found towards the edges of the galaxy. It usually shows a central condensation, which is, however, in most cases not very conspicuous.

Many of these objects have been discovered on the new, second Palomar Observatory Sky Survey plates that are cur-

rently being obtained (SBSM). Some of the objects were already visible on the original POSS plates, but were never catalogued.

LSB galaxies have H I masses of a few times 10^9 $M_\odot$ (van der Hulst et al. 1993; McGaugh 1992; SBSM). Observations with the Westerbork Synthesis Radio Telescope and the Very Large Array show low H I surface densities, usually close to or even below the critical surface density for star formation as formulated by Kennicutt (1989). The oxygen abundances in the few H II regions these galaxies possess are quite low: ~ 0.1 to ~ 0.5 solar metallicity (McGaugh 1994; de Blok & van der Hulst, in preparation). Previous studies have shown that LSB galaxies are unusually blue compared to normal late-type galaxies (McGaugh 1992; van der Hulst et al. 1993; Knezek 1993). So far no CO emission has been detected (Schombert et al. 1990; van der Hulst & de Blok, in preparation). Thuan, Gott & Schneider (1987) and Bothun et al. (1993) find that, although LSB galaxies follow the spatial distribution of HSB galaxies, they tend to be more isolated from their nearest neighbours than HSB galaxies.

If we assume that large amounts of star formation are triggered by major tidal interactions or infall of companions, the above results and the lack of major star formation suggest that LSB galaxies are relatively unperturbed, and have not suffered from these events. These galaxies thus offer a unique opportunity to extend the range of environments in which we can study the properties of galaxies and star formation.

Some LSB galaxies have remarkable characteristics: Malin 1 (Impey & Bothun 1989) has a huge (55 kpc, $H_0 = 100$ km s^{-1} Mpc^{-1}) scale length, a very low central disc surface brightness ($\mu_B(0) \approx 25.5$ mag arcsec^{-2}), and an enormous neutral hydrogen mass ($M_{\rm HI} \sim 10^{11} M_\odot$). Malin 1 is an extreme case, but no exception. Studies by e.g. Knezek (1993) and McGaugh (1992) (but see also McGaugh & Bothun 1994) show that the range in LSB galaxy sizes and H I masses is comparable with that of high surface brightness (HSB) galaxies that define the Hubble sequence.

It should be stressed that the LSB galaxies we study here are *neither* Malin-1-like giant galaxies, *nor* intrinsically small galaxies such as the dwarf ellipticals and dwarf irregulars from our Local Group. As already stated, the LSB galaxies we study resemble normal late-type spirals in their morphology.

Section 2 of this paper will discuss the sample and the reduction techniques. In Section 3 we will show and discuss the results. Section 4 describes the colours in our sample. In Section 5 we will describe the properties of a few individual galaxies. In Section 6 we will compare our data with photometric evolution models from the literature and discuss age- and metallicity-effects. In Section 7 possible star formation histories will be discussed and in Section 8 we will summarize the discussion, and give some concluding remarks.

2 SAMPLE AND REDUCTION

2.1 The sample

We selected 21 galaxies from the lists of LSB galaxies by SBSM and the UGC (Nilson 1973) using the following selection criteria:

(i) $\mu_B(0) > 23$ mag arcsec^{-2},
(ii) single-dish H I observations available,
(iii) estimated inclinations $i < 60°$.

The selected galaxies turned out to be morphologically similar to late Hubble type galaxies (Scd and later). Follow-up synthesis H I observations of the galaxies in our sample are discussed by McGaugh (1992), van der Hulst et al. (1993), and de Blok, McGaugh & van der Hulst (in preparation). It should be noted that the sample discussed by McGaugh (1992) was also selected using the above criteria.

Fig. 1 shows *R*-band images of our sample of LSB galaxies. These images are presented using a linear intensity scale adjusted to bring out the faint outer parts, so that the brighter inner parts are saturated. In most cases this gives the impression that there is a bulge present. This is, however, an artefact of the intensity scale used. Table 1 lists the sample. The distances were derived from the heliocentric redshifts (SBSM). These redshifts were corrected for Galactic rotation and Virgocentric flow, and converted to distances, assuming a Hubble constant $H_0 = 100$ km s^{-1} Mpc^{-1}.

In this table and the rest of this paper all Galactic extinction-corrected magnitudes and colours have been corrected assuming a standard stellar extinction curve, following Allen (1973) and Burstein & Heiles (1982). Extinctions in the *B*-band were furthermore determined using the NED database. As the dust content of LSB galaxies is probably low (McGaugh 1992) and as the optical inclinations have a large uncertainty, we have not corrected for internal extinction in the LSB galaxies. Total magnitudes are given in Table 2, and will be discussed later.

2.2 Observations

UBVRI images of the galaxies in the sample were taken during 4 nights in the period from 1991 January 8 until January 14, with the 2.5-m Isaac Newton Telescope at La Palma. The nights were excellent, with good (~1 arcsec) seeing and mostly photometric conditions. A GEC CCD was used, with a pixel size of 0.54 arcsec.

Images were bias-subtracted, flatfielded and co-added with the MIDAS package using standard methods. Flatfield images had been taken several times each night. Deviations between flats made on different nights using the same filter were $\lesssim 1$ per cent.

2.3 Flux calibration

The images were flux-calibrated using standard stars (Landolt 1983). Since many standard star exposures had been taken through each filter we could compare these to determine the errors in the photometry over the 4 nights. We found these to be 0.04 mag (1σ) for the *U*-filter, based on 19 exposures. The deviation for the *B*-filter was the largest: 0.05 mag, based on 12 exposures. The deviation for the *V*-filter was 0.02 mag, based on 11 exposures. The *R*-filter standard stars showed a deviation of 0.02 mag, based on 17 exposures, and the *I*-filter stars also showed a deviation of 0.02 mag, based on 5 exposures, all of these exposures taken during 4 nights.

2.4 Sky subtraction

To determine the sky background and the errors caused by its subtraction we used the following procedure.

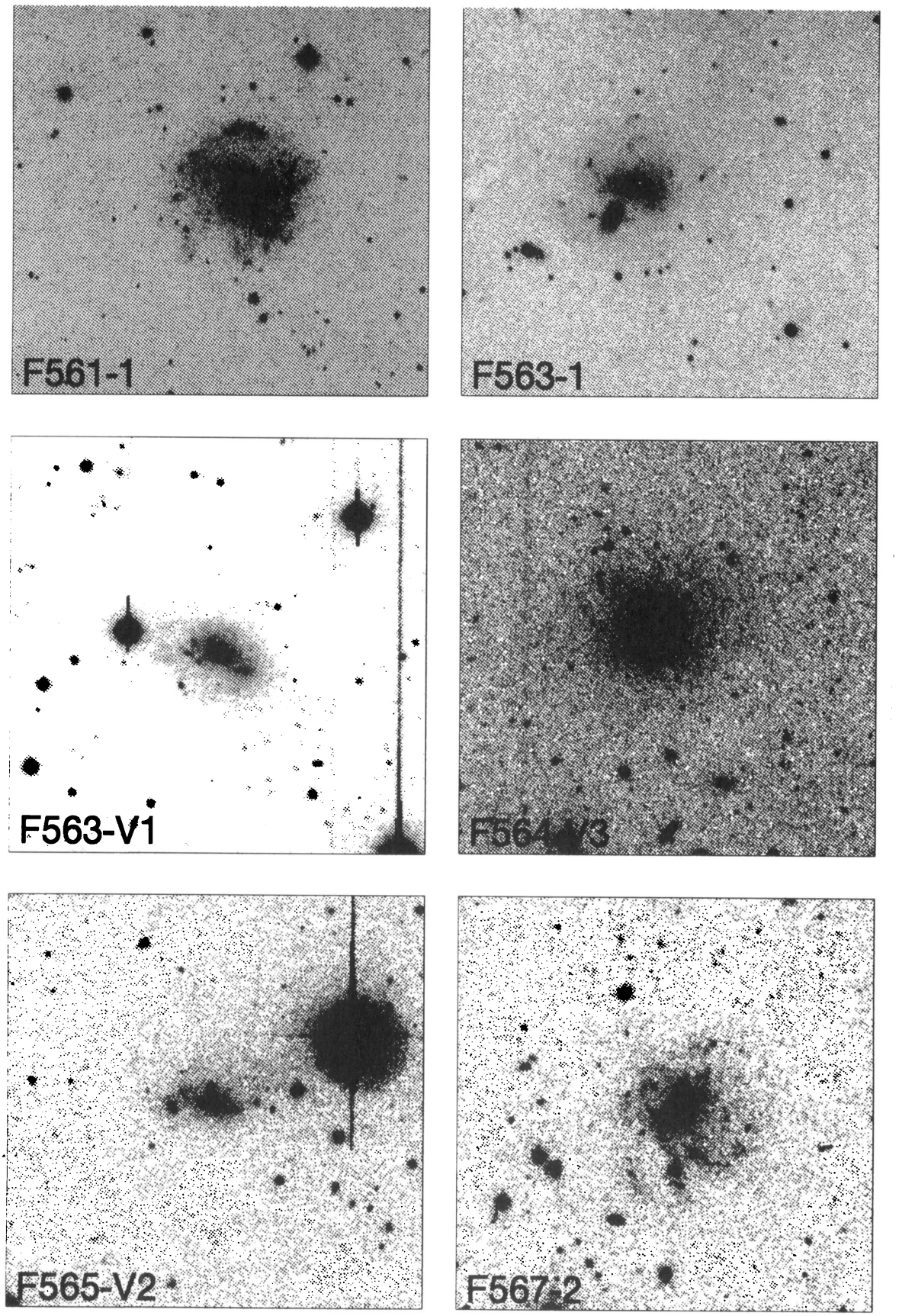

Figure 1. *R*-images of the sample of LSB galaxies. Image sizes are 2.3 × 2.3 arcmin^2. North is at the right, east is at the top. Top-left: F561-1; top-right: F563-1; middle-left: F563-V1; middle-right: F564-V3; bottom-left: F565-V2 bottom-right: F567-2.

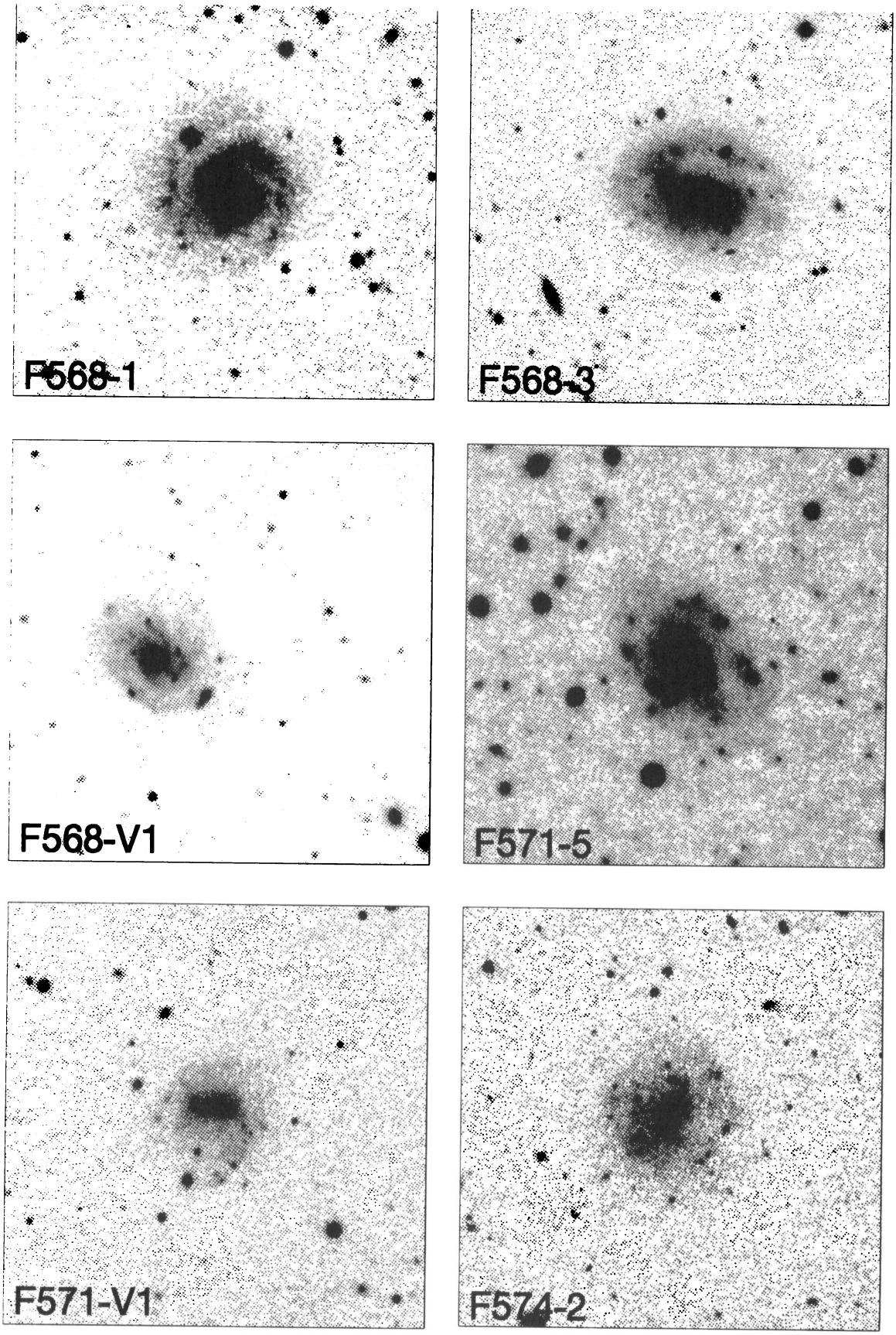

Figure 1 – *continued.* Top-left: F568-1; top-right: F568-3; middle-left: F568-V1; middle-right: F571-5; bottom-left: F571-V1; bottom-right: F574-2.

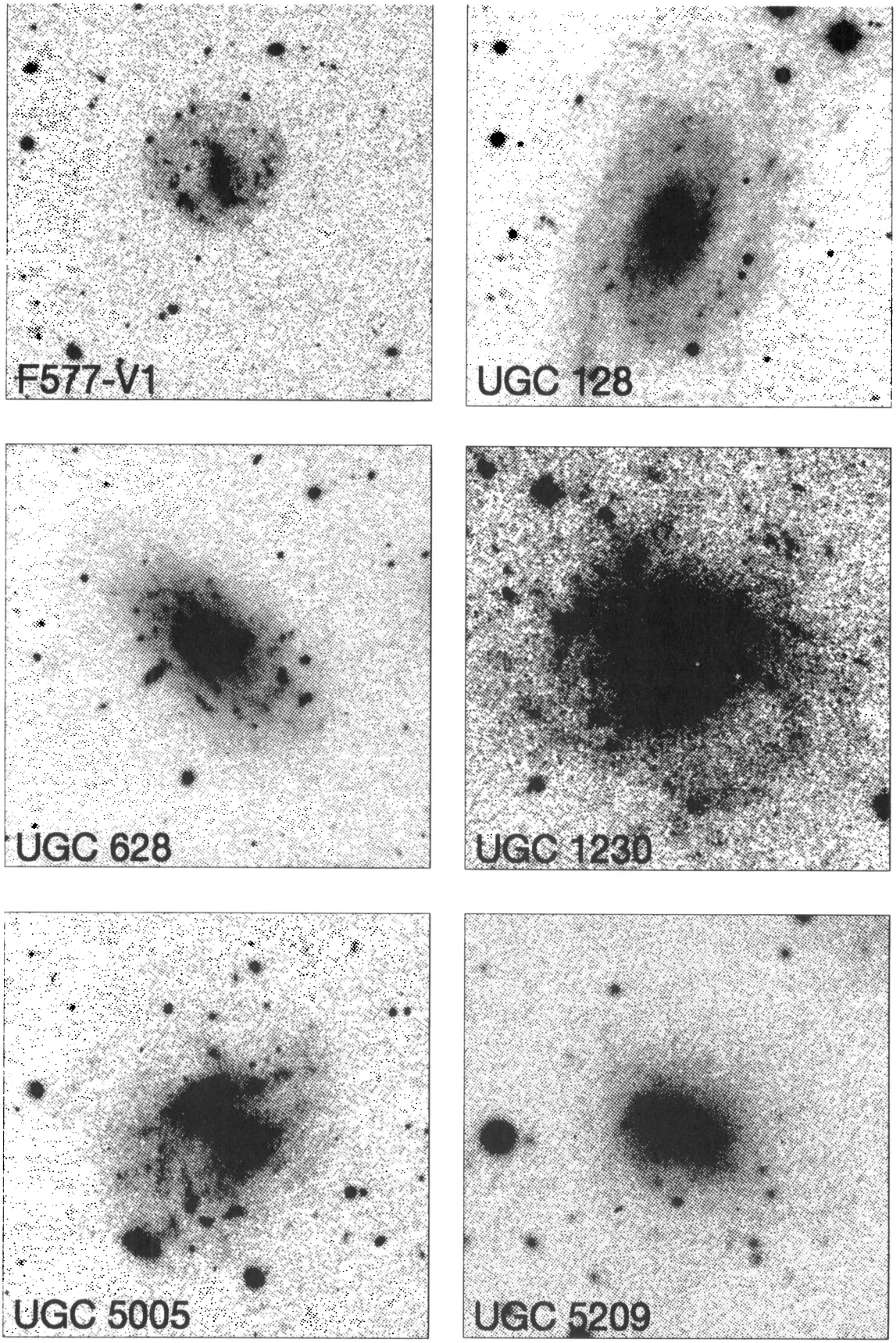

Figure 1 – *continued.* Top-left: F577-V1; top-right: UGC 128; middle-left: UGC 628; middle-right: UGC 1230; bottom-left: UGC 5005; bottom-right: UGC 5209.

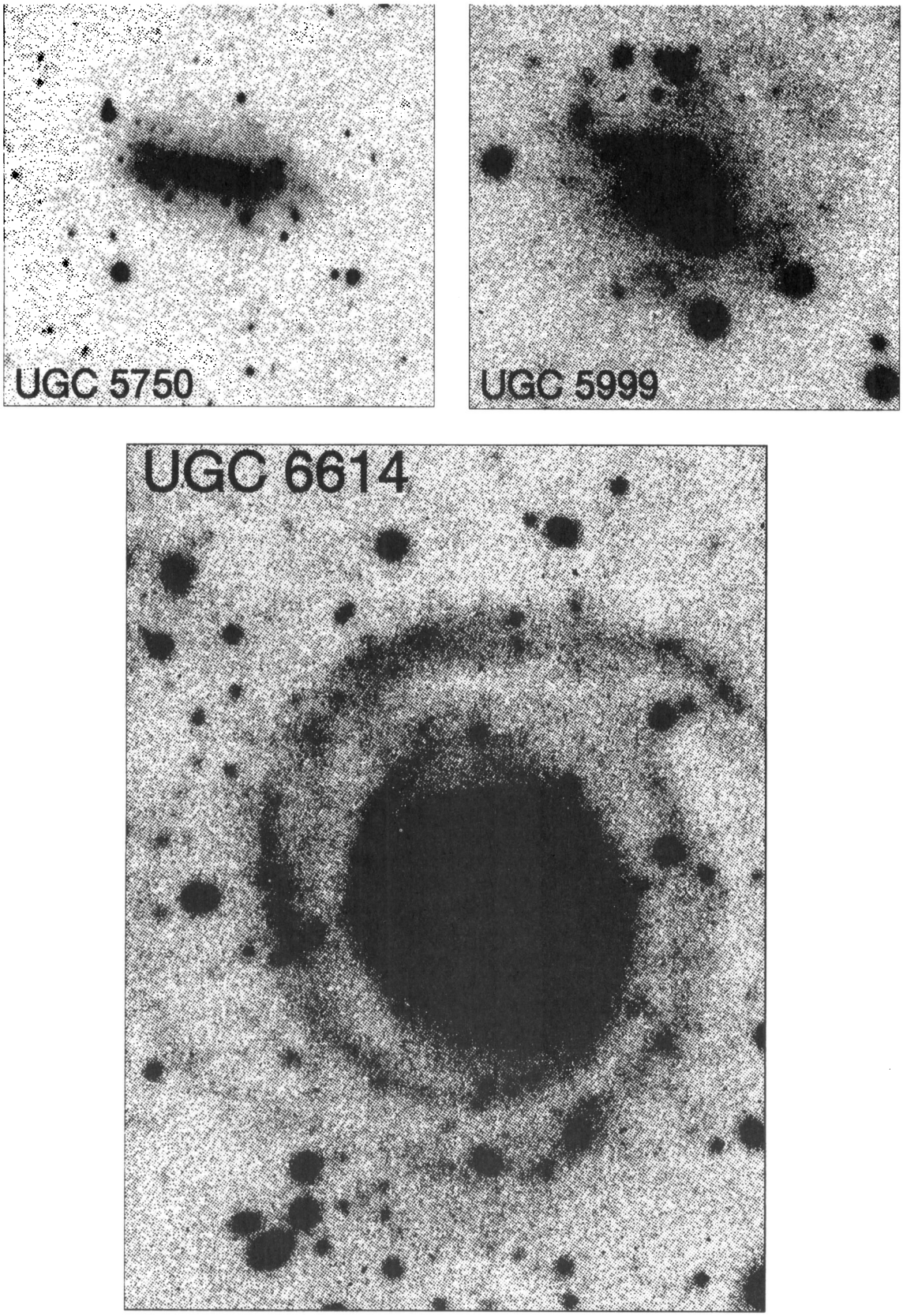

Figure 1 – *continued.* Top-left: UGC 5750; top-right: UGC 5999; bottom: UGC 6614, image size is 3.4 × 3.4 arcmin^2.

Table 1. Parameters of the sample.

(1) Name	(2) α(1950)	(3) δ(1950)	(4) i	(5) D	(6) B_{25}	(7) $r_{B_{25}}$	(8) B_{27}	(9) $r_{B_{27}}$	(10) R_{25}	(11) R_{27}	(12) A_B
F 561-1	08 06 45	+22 42 25	14	47	16.43	21	16.16	29	15.63	15.42	0.11
F 563-1	08 52 10	+19 56 35	52	34	16.77	23	15.90	62	15.96	15.23	0.06
F 563-V1	08 43 48	+19 04 26	42	38	17.98	13	17.26	25	16.46	15.78	0.05
F 564-V3	09 00 03	+20 16 23	26	6	18.35	11	17.09	29	17.47	16.38	0.07
F 565-V2	09 34 47	+21 59 46	64	36	19.28	10	18.10	27	18.57	17.29	0.05
F 567-2	10 15 11	+21 18 47	37	56	18.61	9	17.07	31	17.69	16.41	0.06
F 568-1	10 22 57	+22 40 44	26	64	17.12	18	15.54	31	16.16	15.72	0.02
F 568-3	10 24 15	+22 28 51	39	58	16.45	21	16.15	31	15.54	15.30	0.02
F 568-V1	10 43 44	+22 23 50	35	60	17.20	16	16.69	29	16.28	15.85	0.00
F 571-5	11 27 49	+20 52 10	40	45	17.80	13	16.81	31	17.01	16.19	0.00
F 571-V1	11 23 42	+19 07 56	35	59	18.54	10	17.50	25	17.59	16.64	0.00
F 574-2	12 44 19	+22 04 34	29	66	18.77	9	17.17	27	17.80	16.47	0.14
F 577-V1	13 47 49	+18 30 53	33	80	17.57	17	16.95	29	16.90	16.43	0.01
U 0128	00 11 12	+35 43 00	57	48	15.98	31	15.07	78	15.07	14.36	0.18
U 0628	00 58 18	+19 13 00	56	56	15.84	31	15.56	51	14.91	14.64	0.09
U 1230	01 42 42	+25 16 00	20	40	16.16	21	15.06	62	15.31	14.46	0.40
U 5005	09 21 39	+22 29 20	40	37	–	41R	–	49R	15.01	14.92	0.10
U 5209	09 45 04	+32 14 11	50	7	–	33R	–	62R	15.54	15.21	0.00
U 5750	10 33 02	+21 15 00	61	71	–	35R	–	70R	15.51	15.32	0.02
U 5999	10 50 13	+07 53 13	27	32	–	45R	–	90R	15.11	14.65	0.05
U 6614	11 36 36	+17 25 00	54	66	–	57R	–	>120R	13.08	<12.81	0.02

Note:
(1) Name of the galaxy. 'U' means from the UGC; 'F' means SBSM.
(2) Right Ascension (1950.0) from either UGC or SBSM.
(3) Declination (1950.0) from UGC or SBSM.
(4) Inclination as derived from our data.
(5) Distance in Mpc ($H_0 = 100$ km s^{-1} Mpc^{-1}).
(6) Total magnitude B_{25} within 25 B-mag arcsec^{-2} ellipse.
(7) Radius in arcsec of 25 B-mag arcsec^{-2} ellipse.
(8) Total magnitude B_{27} within 27 B-mag arcsec^{-2} ellipse.
(9) Radius in arcsec of 27 B-mag arcsec^{-2} ellipse.
(10) Total magnitude R_{25} within 25 B-mag arcsec^{-2} ellipse.
(11) Total magnitude R_{27} within 27 B-mag arcsec^{-2} ellipse.
(12) Applied extinction correction in B.
If the values in columns (7) and (9) are followed by an 'R', then these are measured in the R-band.

If the sky background had a significant gradient across the image an attempt was made to fit and remove this gradient, without changing the mean value of the sky background. To do this the brightest stars were first removed from the image, after which the image was Gaussian-smoothed, decreasing its resolution by a factor of two. This removed small-scale noise fluctuations and showed more clearly which parts of the image were affected by the glare of the remaining fainter stars. A two-dimensional first-order polynomial was then fitted to those parts of the smoothed sky background that were judged to be free of any emission from stars or the galaxy itself.

This gradient was then subtracted from the original image, essentially flattening the image background, without affecting the mean value of the sky or the values for the galaxy. We then measured the mean value of the sky background and the standard deviation in small boxes that were placed on parts of the image that were free of stellar or galaxy emission.

The mean difference between the median sky levels in these boxes was used as an estimate for the error introduced by fitting and subtracting the sky. Typically these errors were less than 0.5 per cent of the subtracted sky level.

2.5 Ellipse fitting and inclinations

We used the GIPSY image processing package to make ellipse fits to the isophotes of the galaxies, and to integrate along these ellipses. The centres of the ellipses were usually determined by taking the maximum of the light distribution as the centre. In one or two cases the light distribution was too irregular and the central position was taken as a free parameter in the ellipse fit. For each set of *UBVRI* images of an object only one set of ellipse orientation parameters was determined (usually from a slightly smoothed R-image), and applied to the other images to get radial azimuthally integrated surface brightness profiles for each band. As the galaxies did not contain any significant bulges or strong bars that might twist the isophotes, we fitted ellipses with constant axial ratios, centres and position angles where the axial ratios and position angles were determined by the outer isophotes. These outer isophotes give the best idea of the overall shape of the galaxy. Prior to the fitting, stars and cosmic ray defects were first blanked. As an extra check a few images were also fitted using a free parameter fitting routine, with no constraints on the axial ratio or orientation, and resulted in virtually identical radial surface brightness profiles.

Inclinations were derived from these ellipse fits, using $\cos i = (b/a)$, and corrected for the intrinsic thickness of the disc by using the following formula from Holmberg (1958):

$$\cos^2 i = \frac{(b/a)^2 - q_0^2}{1 - q_0^2} \quad (1)$$

where q_0, the edge-on axial ratio of the disc, is taken to be 0.15 (cf. Huizinga 1994; Giovanelli et al. 1994).

3 SURFACE BRIGHTNESS, SCALE LENGTH AND HUBBLE TYPE

3.1 The data

The surface brightness profiles of LSB galaxies can be very well approximated by an exponential disc component of the form

$$\Sigma(r) = \Sigma_0 \exp\left(-\frac{r}{h}\right), \quad (2)$$

where Σ_0 is the surface brightness of the disc in linear units ($M_\odot$ pc^{-2}), and h is the exponential scale length of the disc (de Vaucouleurs 1959). This equation can be converted to logarithmic units:

$$\mu(r) = \mu_0 + 1.086\left(\frac{r}{h}\right), \quad (3)$$

where μ_0 is the central surface brightness of the disc in logarithmic units (mag arcsec^{-2}).

Fig. 2 shows the azimuthally integrated radial surface brightness profiles of the galaxies in our sample for the *B*- and *R*-bands. It is clear from Figs 1 and 2 that most of the galaxies in our sample do not have significant bulges.

The central surface brightness μ_0 of the disc and the exponential major axis scale length h were found by fitting a straight line to the exponential part of the profile, where the inner few points were excluded from the fit.

Table 2 shows the fit parameters, along with other parameters derived from them. We have not corrected the central disc surface brightness in Column (3) to face-on value as the optical depth effects in LSB galaxies are not known. We suspect LSB galaxies to have a low dust content (see McGaugh 1992 and Section 3.4). The mean error in the central surface brightness is about 0.1 mag arcsec^{-2} and the mean error in the scale length is $\sim$ 20 per cent. These errors are derived from the error in the fit and the error bars in the outer points, which are in turn mainly determined by the error due to sky subtraction. The total integrated magnitude of the disc, integrated out to infinity, as given in Column (6) is calculated using

$$m_T = \mu_0 - 2.5\log(2\pi h^2) - 2.5\log(\cos i), \quad (4)$$

where the last term corrects the area of a face-on disc to the apparent area of an inclined disc. The method used to determine the simulated aperture photometry magnitudes in Column (7) is described in Section 3.2. All magnitudes in this and other tables are corrected for Galactic foreground extinction, as described in Section 2.1.

3.2 Total magnitudes

The conventional m_{25} magnitude, which gives the amount of light within the 25 mag arcsec^{-2} isophote, is not a good measure for the total luminosity of LSB galaxies. In HSB galaxies most of the light is concentrated within this isophote ($\sim$ 80 per cent), but this is not the case for LSB galaxies. F565-V2, for example, has a central *B*-surface brightness of $\sim$ 24.5 mag arcsec^{-2} and a scale length of 2 kpc. Assuming a purely exponential light distribution, this means that only 8 per cent of the light of this galaxy is emitted within the 25 mag arcsec^{-2} isophote. The total magnitude out to infinity m_T, as defined by equation (4), is a better estimate for the total luminosity of a LSB galaxy. It is, however, difficult to get very accurate values for m_T, as they do depend on an extrapolation of the scale length, thus introducing extra uncertainties. Isophotal magnitudes are determined directly from the data and do not depend on extrapolations.

In our sample we can trace the galaxies out to a surface brightness of $\sim$ 28 mag arcsec^{-2} in *B* ($\sim$ 3.5 scale lengths). Assuming that our galaxies are perfect exponential discs, this implies that we have detected more than 90 per cent of the total light. The data are thus good enough to determine the total magnitude directly. We have done this by using curves of growth to simulate aperture photometry. The magnitude m_{apt} we derive is a better estimate for the total magnitude than m_T. It takes any central surplus non-disc light into account, and no extra light is introduced at very large radii. Also for m_{apt} the errors in the magnitudes are still mainly determined by the errors in the sky subtraction.

It is instructive to compare m_{25} with m_{apt}, the amount of light within the maximum aperture radius. This is done in Fig. 3. It is clear that m_{25} underestimates the amount of light present. Therefore, one should be careful in using m_{25} to calculate, for example, mass-to-light ratios, since use of m_{25} will artificially raise this ratio, and more so in LSB galaxies. For example, a LSB galaxy with $\mu_B(0) = 24.5$ mag arcsec^{-2} and a scale length of 2 kpc has 10 times less light within the 25 *B*-mag arcsec^{-2} isophote than a HSB galaxy with a central surface brightness equal to the Freeman value. Its mass-to-light ratio will therefore artificially be 10 times higher when m_{25} is used, even though these galaxies may have the same mass and total luminosity.

3.3 Surface brightnesses and scale lengths

Fig. 4 shows the distributions of central disc surface brightnesses and scale lengths. The median values for our sample are $\mu_B(0) = 23.6$ mag arcsec^{-2} and $h = 3.2$ kpc. Combination of our data with those of McGaugh* (1992, his fig. 2.3) yields median values of respectively 23.4 mag arcsec^{-2} and 3.2 kpc. The median of the surface brightness is thus shifted more than 6σ from the Freeman (1970) value $\mu_B(0) = 21.65 \pm 0.30$ mag arcsec^{-2}.

The peaked distribution in the central surface brightness histogram (Figs 4c and d) is caused by two effects. The upper cut-off in the histogram is due to a selection criterion of the sample: objects with central blue surface brightnesses brighter than 23 mag arcsec^{-2} were excluded†. The lower cut-off is

* The selection criteria of the sample in McGaugh are identical to ours (see Section 2.1), and a direct comparison is valid.

† When measured with a CCD some central surface brightnesses were found to be a few tenths of a magnitude brighter, hence the galaxies which have $\mu_B(0) < 23$ mag arcsec^{-2}.

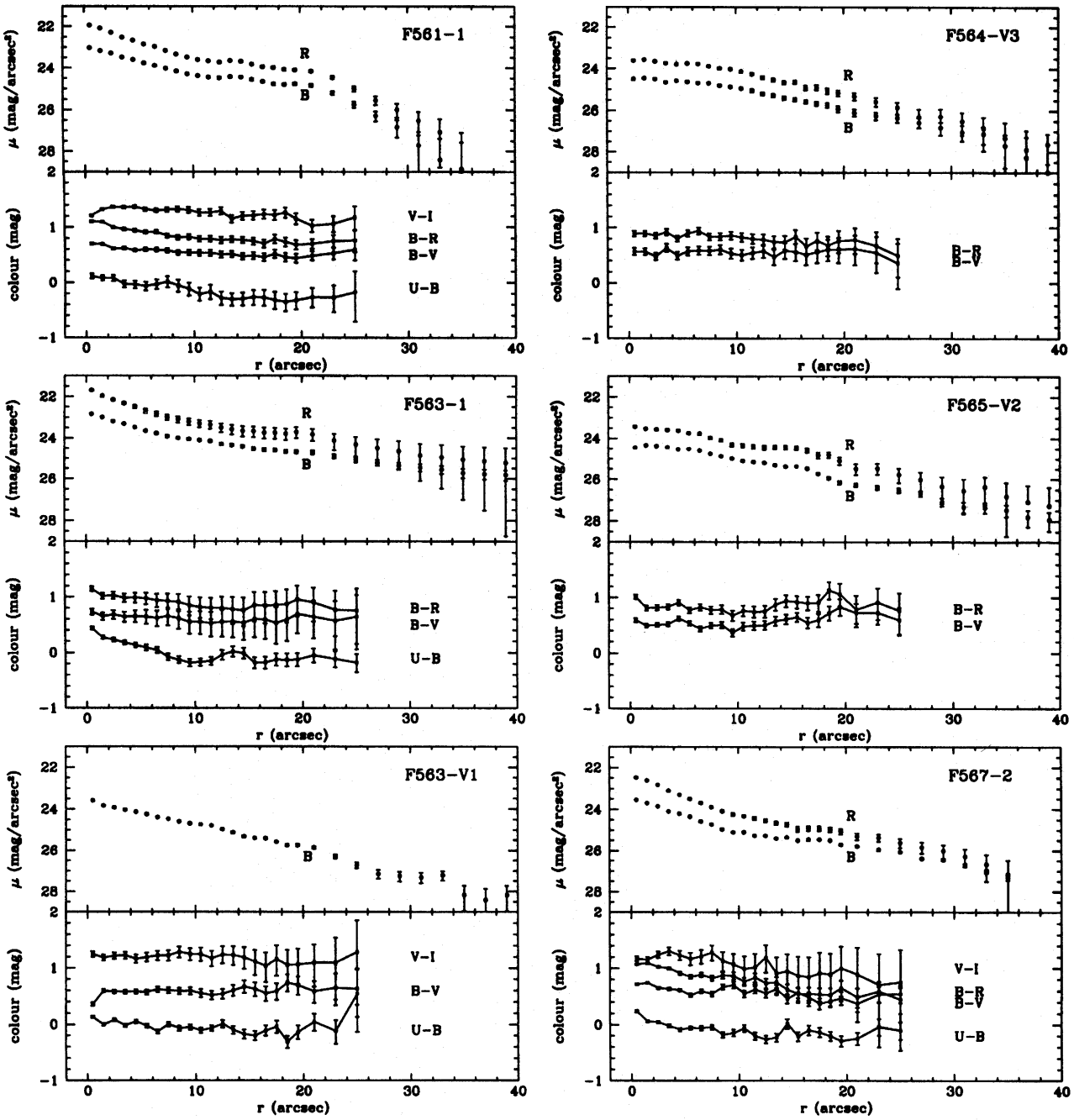

Figure 2. Radial surface brightness and colour profiles. Top panels contain B (lower profile) and R (upper profile) surface brightness profiles; bottom panels contain radial colour profiles (where measured). In all cases $V-I$ has been offset by +0.5 mag. For some UGC galaxies no colour profiles are available, and only the R-band profile is given.

caused by the detection limit of the plates and the diameter limits imposed on the SBSM sample.

The range in surface brightness in the histogram is large and reaches from ~ 24.5 mag arcsec^{-2} to close to the Freeman value: a factor of 10 in luminosity surface density.

The range of scale lengths found is virtually indistinguishable from that found for complete samples of HSB spiral galaxies (van der Kruit 1987; Grosbøl 1985). The HSB galaxies investigated in these studies have scale lengths varying from 1 to 6 kpc. The LSB galaxies investigated here and in McGaugh (1992) have scale lengths in the same range.

3.4 Central surface brightnesses and Hubble types

The Hubble sequence is based on different galaxies having different properties. Early-type spiral galaxies are found to have large bulges, a small gas fraction, and redder discs, while late-type spiral galaxies have small or no bulges, a large gas fraction, and bluer discs. Our LSB galaxies are classified as very late-type galaxies with Hubble types between Sd and Im (cf. SBSM). We will show in the following that LSB galaxies are always among the faintest galaxies for each Hubble type.

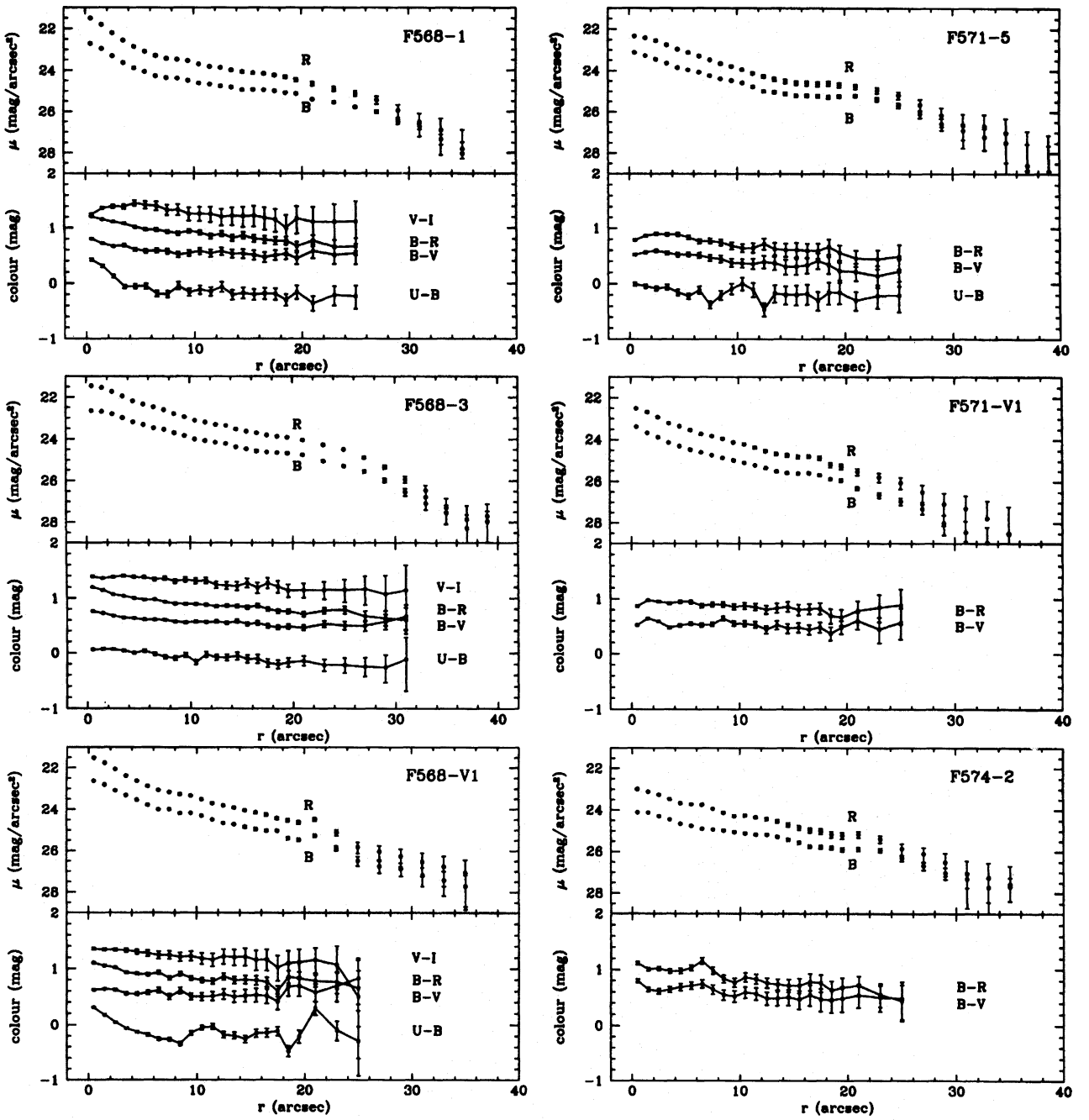

Figure 2 – *continued*

One of the largest galaxy catalogues with photometric information is the ESO-LV catalogue (Lauberts & Valentijn 1989). We selected a subsample from this catalogue to represent the Hubble sequence using the following criteria. First we selected only those galaxies with revised Hubble types between 0 and 10 inclusive (S0 to Irr). To avoid extinction and optical depth effects we also rejected all galaxies with inclinations $i > 50°$, and galactic latitude $|b| < 15°$. These criteria resulted in a sample of about 12000 galaxies. The method that was used in the ESO-LV to determine central surface brightnesses is different from our method, so, instead of using the ESO-LV central surface brightnesses, we decided to use the effective surface brightness in the B-band, μ_B^e, as given in the ESO-LV.

In order to determine μ_B^e for our LSB galaxies we assumed them to be pure exponential discs with parameters given in Table 2. Figs 1 and 2 show that this is a valid assumption. For an exponential disc a simple calculation yields

$$\mu_B^e = \mu_B(0) + 1.822. \quad (5)$$

Fig. 5 shows the distribution of μ_B^e with Hubble type (as given in SBSM). The small dots show the individual ESO-LV galaxies; the large circles with error bars represent the mean effective surface brightness for each Hubble type bin with 1σ error bars. It is clear that the general trend is that surface brightness becomes fainter with Hubble type.

We think it is unlikely that this decrease is caused entirely

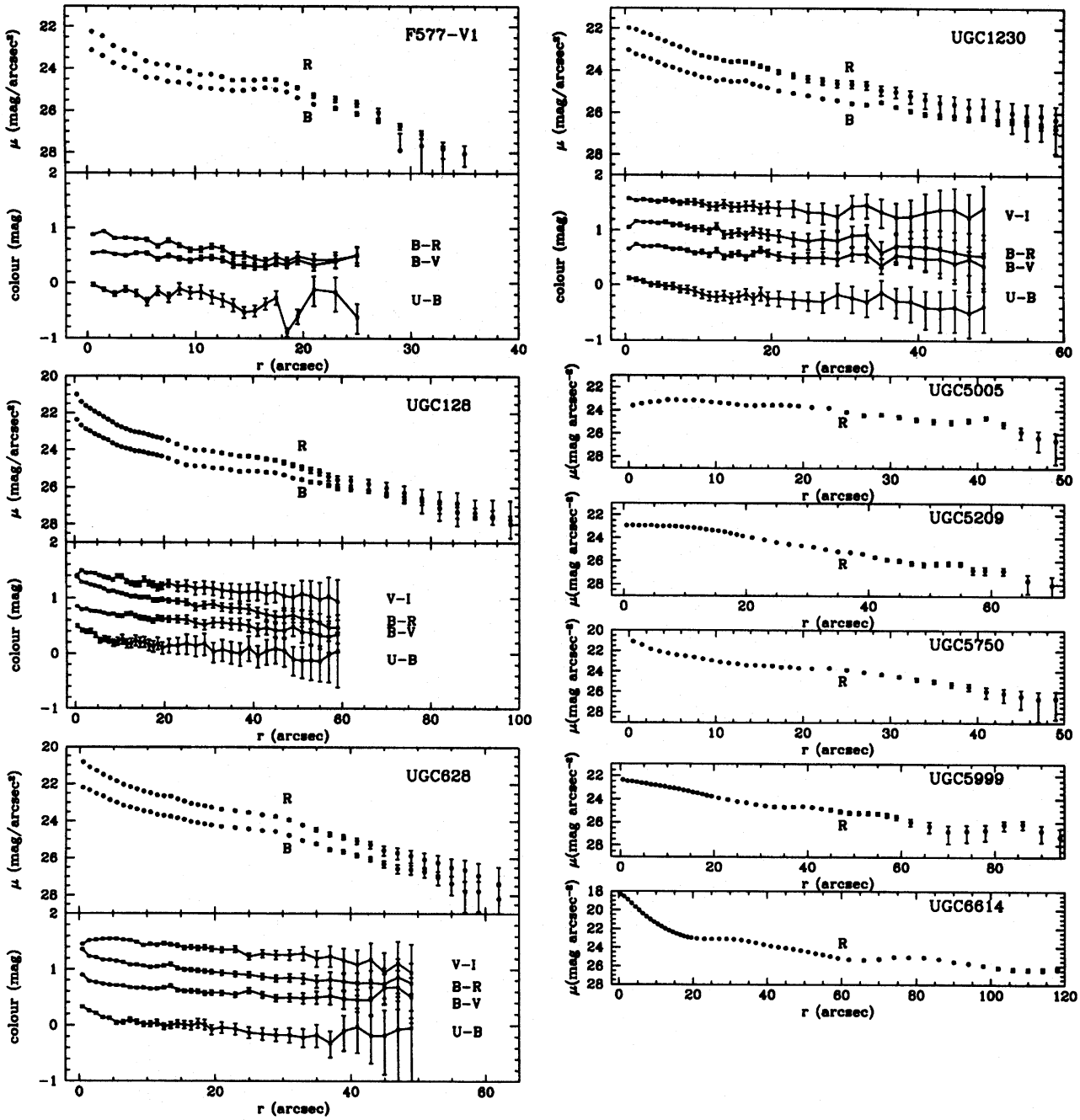

Figure 2 – *continued*

by dust. The following results indicate that the dust content of LSB galaxies is low.

(i) The Balmer decrements towards H II regions in LSB galaxies are found to be very small (McGaugh 1992; de Blok & van der Hulst, in preparation), thus suggesting that the amount of dust in the line of sight towards these H II regions is small.

(ii) No CO has yet been detected in these galaxies (Schombert et al. 1990; de Blok & van der Hulst, in preparation). The best 3σ upper limits for CO emission in LSB galaxies are $T_b \sim 3$ mK at a velocity resolution of 10 km s^{-1}. These low amounts of CO, together with the low metallicities in these galaxies (McGaugh 1992), also suggest a low dust content.

Hence we consider it unlikely that dust alone is responsible for the trend of decreasing surface brightness with Hubble type. Furthermore, this trend is also present in the near-infrared, where extinction effects are less severe (Peletier & Willner 1993). The big black dots represent our sample of LSB galaxies, where equation (5) was used to determine μ_B^e and the Hubble types were taken from SBSM.

We see that, as far as the late-type LSB galaxies are concerned, almost all of the LSB galaxies lie higher (fainter) than the main portion of the Hubble sequence. So at each Hubble type the LSB galaxies are among the faintest galaxies for that Hubble type. The range in physical properties at each Hubble type is too large to use the Hubble type as a single classifying parameter.

Table 2. Scale lengths and magnitudes of LSB galaxies.

Name (1)	band (2)	μ_0 (3)	h (4)	h' (5)	m_T (6)	m_{apt} (7)	M_T (8)	Name (1)	band (2)	μ_0 (3)	h (4)	h' (5)	m_T (6)	m_{apt} (7)	M_T (8)
F561-1	U	23.10	12.19	2.8	15.70	15.94	-17.42	F568-V1	U	22.81	8.54	2.5	16.38	16.53	-17.36
	B	23.19	11.91	2.7	15.84	16.15	-17.21		B	23.01	8.20	2.4	16.67	16.63	-17.26
	V	22.48	10.93	2.5	15.32	15.56	-17.80		V	22.78	10.49	3.1	15.90	16.12	-17.77
	R	22.39	11.59	2.6	15.10	15.38	-17.98		R	22.52	10.18	3.0	15.71	15.85	-18.04
	I	21.75	10.46	2.4	14.69	14.93	-18.43		I	21.96	9.27	2.7	15.72	15.42	-18.47
F563-1	U	23.07	15.11	2.5	15.71	16.08	-16.59	F571-5	U	23.10	8.64	1.9	16.71	16.62	-16.64
	B	23.53	19.67	3.2	15.60	15.96	-16.71		B	23.37	10.15	2.2	16.63	16.75	-16.52
	V	23.21:	25.06:	4.1	14.75	15.30	-17.36		V	22.81	9.05	2.0	16.32	16.41	-16.86
	R	22.47:	15.88	2.6	15.00	15.31	-17.35		R	22.74	10.20	2.2	15.99	16.15	-17.12
	I	22.91	11.89	2.0	16.07	16.25	-16.41	F571-V1	B	23.78	8.35	2.4	17.40	17.43	-16.42
F563-V1	U	23.44	9.59	1.8	16.86	17.19	-15.71		V	23.18	8.41	2.4	16.78	16.90	-16.95
	B	23.54	9.72	1.8	16.93	17.16	-15.74		R	22.85	8.10	2.3	16.69	16.55	-17.30
	V	23.06	10.34	1.9	16.31	16.60	-16.30	F574-2	B	24.19	14.03	4.5	16.61	17.08	-17.02
	R	22.07::	9.43	1.7	15.52	15.64	-17.26		V	23.52	13.11	4.2	16.09	16.46	-17.65
	I	22.24	8.95	1.7	15.81	15.98	-16.92		R	23.19	11.73	3.8	16.00	16.35	-17.75
F564-V3	B	23.89	11.22	0.3	16.76	16.98	-11.77	F577-V1	U	23.66	12.63	4.9	16.35	16.60	-17.92
	V	23.10	9.56	0.3	16.32	16.48	-12.41		B	23.73	11.09	4.3	16.70	16.93	-17.59
	R	22.96	9.81	0.3	16.13	16.29	-12.60		V	23.14	10.33	4.0	16.26	16.55	-17.97
F565-V2	B	23.98	11.53	2.0	17.58	18.00	-14.79		R	23.09	10.52	4.1	16.17	16.40	-18.12
	V	23.46	11.55	2.0	17.05	17.47	-15.32	U0128	U	24.03	44.41	10.3	13.87	14.94	-18.47
	R	23.08	10.65	1.9	16.85	17.23	-15.55		B	23.57	29.60	6.9	14.29	15.25	-18.16
F567-2	U	24.19	16.29	4.4	16.37	16.75	-16.99		V	22.91	25.93	6.0	13.92	14.78	-18.67
	B	24.35	15.77	4.3	16.61	16.98	-16.76		R	22.38	21.90	5.1	13.75	14.56	-18.85
	V	23.69	13.14	3.6	16.34	16.31	-17.43		I	22.04	21.51	5.0	13.45	14.17	-19.25
	R	23.38	11.99	3.3	16.23	16.37	-17.37	U0628	U	22.70	17.94	4.9	15.10	15.24	-18.50
	I	23.05	11.90	3.3	15.92	16.06	-17.68		B	22.50	14.22	4.0	15.40	15.20	-18.54
F568-1	U	23.72	15.67	4.9	15.87	16.37	-17.66		V	22.03	14.18	3.9	14.94	14.64	-19.10
	B	23.65	12.86	4.0	16.23	16.53	-17.50		R	21.50	12.98	3.5	14.60	14.42	-19.32
	V	23.08	12.59	3.9	15.70	15.91	-18.12		I	20.62	10.57	2.9	14.56	14.03	-19.71
	R	22.62	10.67	3.3	15.60	15.74	-18.29	U1230	U	23.19	24.56	4.8	14.87	15.14	-18.87
	I	22.32	12.17	3.8	15.02	15.22	-18.82		B	23.30	20.61	4.0	15.36	15.30	-17.71
F568-3	U	22.83	11.24	3.2	15.85	16.01	-17.80		V	22.85	19.79	3.8	15.00	14.78	-18.23
	B	22.79	10.76	3.0	15.91	16.12	-17.69		R	22.54	17.72	3.4	14.43	14.54	-18.47
	V	22.24	10.49	3.0	15.41	15.57	-18.24		I	22.01	18.40	3.6	14.32	14.10	-18.91
	R	22.17	11.97	3.4	15.05	15.28	-18.53	U5005	R	22.58	18.67	3.3	14.86	14.91	-17.93
	I	21.04	8.37	2.4	14.70	14.83	-18.98	U5209	R	22.33	14.40	0.5	14.83	15.19	-14.04
								U5750	R	21.80	12.23	4.2	14.85	15.42	-18.83
								U5999	R	22.53	20.33	3.2	14.78	14.76	-17.77
								U6614	U	23.55	32.36	10.4	14.58	14.08	-20.02
									R	22.25	29.79	9.5	13.46	12.81	-21.28

Notes:
(1) Name of the galaxy. 'U' means from UGC; 'F' from SBSM.
(2) Photometric band.
(3) Central disc surface brightness in mag arcsec^{-2}.
(4) Exponential scale length in arcseconds.
(5) Exponential scale length in kpc.
(6) Total magnitude of disc, integrated out to infinity. See Section 3.1.
(7) Total magnitude of galaxy, derived from simulated aperture photometry. See Section 3.1.
(8) Total absolute magitude of galaxy, derived using column (7).
Magnitudes and surface brightnesses are corrected for Galactic extinction.

4 COLOURS

4.1 Colour profiles

The colour profiles were determined by subtracting the surface brightness profiles from each other. Four colours were chosen: $U-B$, $B-V$, $B-R$ and $V-I$. The lower panels in Fig. 2 show the radial colour profiles of the galaxies. The errors in the colour profiles were estimated by adding in quadrature the errors in the surface brightness profiles.

To show that the gradients that are seen in most galaxies are real and not a product of the azimuthal integration we show a representative set of colour maps of the LSB galaxies F561-1 and UGC 128 in Fig. 6. Two-colour mapping of galaxies using CCD data has been fully described by Bothun (1986). The goal of this procedure is to show the spatial structure of the galaxy as a function of colour, over wide colour ranges. For the sample here, we have chosen the passbands B and R because this represents the optimal combination of

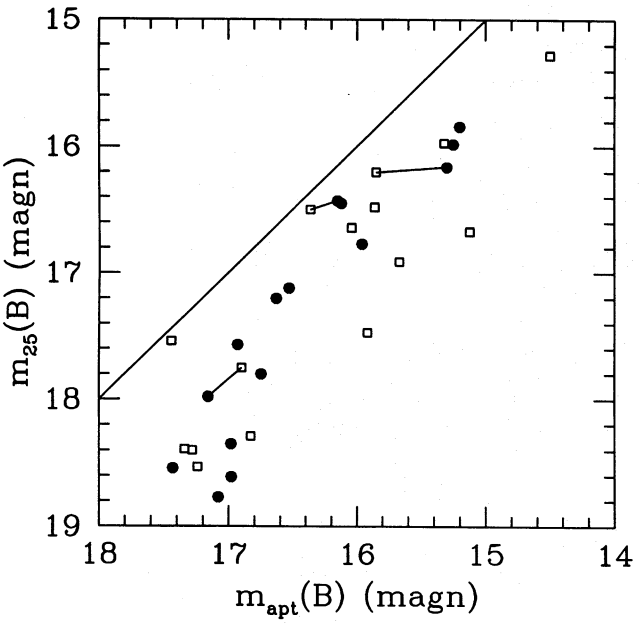

Figure 3. Magnitude within 25 B-mag arcsec^{-2} isophote, $m_{25}(B)$, plotted against aperture magnitude in B, $m_{apt}(B)$. The black circles represent our sample. The open squares represent the sample of McGaugh (1992). Galaxies common to both samples are connected.

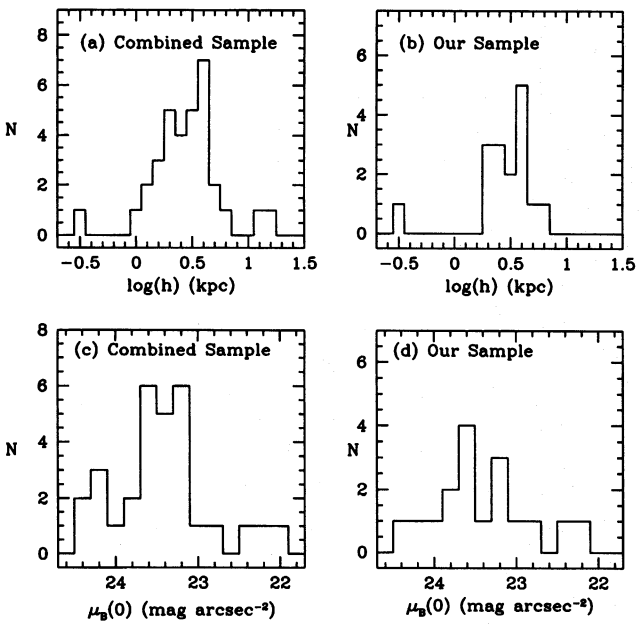

Figure 4. (a) Histogram of the distribution in scale length of the combined sample. (b) Histogram of the distribution in scale length of our sample. (c) Histogram of the distribution in central surface brightness of the combined sample. (d) Histogram of the distribution in central surface brightness of our sample.

signal-to-noise ratio and colour baseline. Average B- and R-surface brightnesses were measured in boxes of size 7×7 pixels. Boxes where the combined error in $B-R$ exceeded 0.07 mag were rejected. Typically several hundred boxes passed the error threshold criteria, and in fact the median error per galaxy is 0.04 mag per box. The errors are entirely dominated by the noise of the R-band sky. The spatial positions of all boxes that pass this error threshold (i.e., with errors in $B-R$ smaller than 0.07 mag) were then plotted as a function of $B-R$ colour. A colour bin width of 0.2 mag was chosen for the different panels to help ensure that we are recording the spatial position of significant colour differences. Fig. 6 thus indicates which parts of the galaxies fall in each of four $B-R$ bins and so demonstrates the very systematic change of colour with radius.

Table 3 gives the gradients in the colour profiles per B-scale length as derived from Fig. 2 and the distances in Table 1. The gradients were determined by making a least-squares fit to the linear part of the profile as shown in Fig. 2. Usually the inner few points had to be excluded as seeing effects or nuclear colours dominated here. In Table 3, Column 1 gives the name of the galaxy, and Columns 2, 4, 6 and 8 give the gradient per B-scale length in respectively $U-B$, $B-V$, $B-R$, and $V-I$. Columns 3, 5, 7 and 9 give the corresponding errors in the gradients.

It is clear that many of the galaxies show a colour gradient, which is usually strongest in $U-B$. The outer parts of the disc are bluer than the inner parts.

The large gradient in $U-B$ of F563-1 is probably caused by the large bright region near the centre of the galaxy which is prominent in U (see Figs 1 and 2).

4.2 Total colours

To determine total colours, all images were smoothed first, decreasing their original resolution by a factor of two to reduce the noise. For each galaxy the smoothed images were divided by each other, excluding pixels less than 2σ from the sky levels, resulting in images showing the distribution of colour.

Three different types of colour were determined.

(i) *nuclear colour:* colour within a central ellipse with major axis of 5 arcsec. The nuclear colour shows the colour of the central part of the disc. It includes light from the bulge or central condensation.

(ii) *luminosity-weighted colour:* average colour of the entire galaxy within the isophote that is 2σ above sky level. This isophote had approximately the same value for all galaxies, and turned out to be the ~ 25.5 B-mag arcsec^{-2} isophote.

(iii) *area-weighted colour:* average colour of the entire galaxy, within the 25.5 B-mag arcsec^{-2} isophote, calculated by first computing the colour of each pixel in the galaxy, and then taking the mean of all colour pixel values. As pixel values less than 2σ above sky were blanked, the value of this parameter does not diverge.

In the case of a disc with a constant surface brightness at all positions the luminosity- and area-weighted colours are equal. However, when determining the luminosity-weighted colour most weight is given to the colours of the luminous and bright parts of a galaxy. This is in contrast with the area-weighted colour where all parts of the galaxy have equal weights, and only the area matters. The difference between area- and luminosity-weighted colours is almost completely determined by the relative strength of the redder inner parts with respect to the bluer outer parts. This is important even in galaxies that show no appreciable bulge, as a pure exponential disc already contains half of its light within 1.68 scale lengths. The area-weighted colour is therefore the best indicator for the

Table 3. Colour gradients per B-scale length h_B in LSB galaxies.

Name	$\Delta(U-B)$ per h_B	error	$\Delta(B-V)$ per h_B	error	$\Delta(B-R)$ per h_B	error	$\Delta(V-I)$ per h_B	error
F561-1	−0.30	0.14	−0.11	0.08	−0.19	0.08	−0.14	0.16
F563-1	−1.15	0.22	−0.06	0.13	−0.16	0.13	–	–
F563-V1	−0.09	0.11	+0.04	0.07	–	–	−0.07	0.13
F564-V3	–	–	−0.05	0.07	−0.10	0.06	–	–
F565-V2	–	–	+0.12	0.08	+0.16	0.06	–	–
F567-2	−0.21	0.17	−0.09	0.13	−0.47	0.13	−0.47	0.22
F568-1	−0.12[a]	0.16	−0.12	0.08	−0.28	0.08	−0.24	0.16
F568-3	−0.12	0.12	−0.09	0.06	−0.15	0.06	−0.12	0.15
F568-V1	−0.07[b]	0.10	−0.07	0.05	−0.12	0.05	−0.10	0.10
F571-5	−0.09	0.11	−0.18	0.07	−0.20	0.07	–	–
F571-V1	–	–	−0.05	0.05	−0.10	0.05	–	–
F574-2	–	–	−0.18	0.09	−0.32	0.09	–	–
F577-V1	−0.17	0.13	−0.09	0.09	−0.26	0.09	–	–
U0128	−0.21	0.35	−0.21	0.21	−0.35	0.21	−0.21	0.35
U0628	−0.16	0.16	−0.12	0.12	−0.16	0.08	−0.16	0.2
U1230	−0.20	0.20	−0.12	0.16	−0.24	0.12	−0.12	0.24

[a] Points with $r < 4$ arcsec are excluded.
[b] Points with $r < 5$ arcsec are excluded.

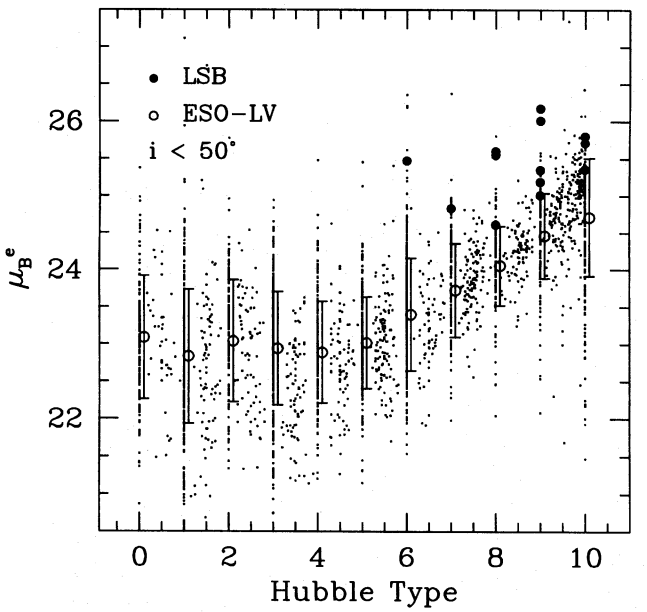

Figure 5. Distribution of the effective surface brightness in B, μ_B^e, as a function of revised Hubble type. The small dots represent the individual galaxies from our ESO-LV sample. The big open circles and error bars represent the mean values and 1σ deviations of μ_B^e for each Hubble type bin. The black dots represent our sample of LSB galaxies.

underlying colours of the disc, while the luminosity-weighted colour is best for comparison with colours derived using aperture photometry.

Table 4 shows these colours corrected for Galactic extinction (see Section 2.1). Errors in these colours are ~ 0.1 mag (based on the errors in the sky subtraction). Column 1 gives the name of the galaxy. Columns 2, 3 and 4 give the nuclear, luminosity-weighted and area-weighted $U-B$ colours, respectively. Columns 5, 6 and 7 give the nuclear, luminosity-weighted and area-weighted $B-V$ colours. Columns 8, 9 and 10 give the nuclear, luminosity-weighted and area-weighted $B-R$ colours. Columns 11, 12 and 13 give the nuclear, luminosity-weighted and area-weighted $V-I$ colours. Column 14 gives the maximum radius in arcseconds that was used to determine the luminosity-weighted and area-weighted colours, and is therefore the radius that corresponds roughly with the 25.5 B-mag arcsec^{-2} isophote.

In Fig. 7 we show the area-weighted $B-V$ colours and structural parameters of the discs with respect to each other. In these figures values found by McGaugh (1992) for his LSB galaxies are also plotted. Among the LSB galaxies there is no trend of colour with surface brightness, although LSB galaxies are bluer than very late-type HSB galaxies. The colours do not depend on the size (scale length) of the galaxy as Fig. 7 shows.

In Fig. 8 we have plotted the average $B-R$ colours of all Sa, Sb, Sc and Sd galaxies in our ESO-LV sample (see Section 3.4) versus the mean effective surface brightness μ_B^e. The filled squares represent the mean values for each Hubble type; the error bars are 1σ error bars. It is clear that LSB galaxies, which are represented by the triangles, are significantly bluer in $B-R$ than late-type HSB galaxies. Our LSB galaxies thus occupy an extreme position in the colour–surface brightness diagram. Combined with Fig. 5 this suggests that for a given Hubble type there is a large range in colour and surface brightness, where LSB galaxies are always among the bluest and faintest galaxies. So characteristics such as colour and surface brightness do not correspond uniquely to Hubble type. This strongly suggests that the Hubble type does not have a one-to-one correspondence with the star formation history, as evidently the star formation history of a late-type LSB galaxy must differ from that of a late-type HSB galaxy.

5 INDIVIDUAL GALAXIES

We will discuss some interesting galaxies in our sample individually. Values for colours and gradients are taken from

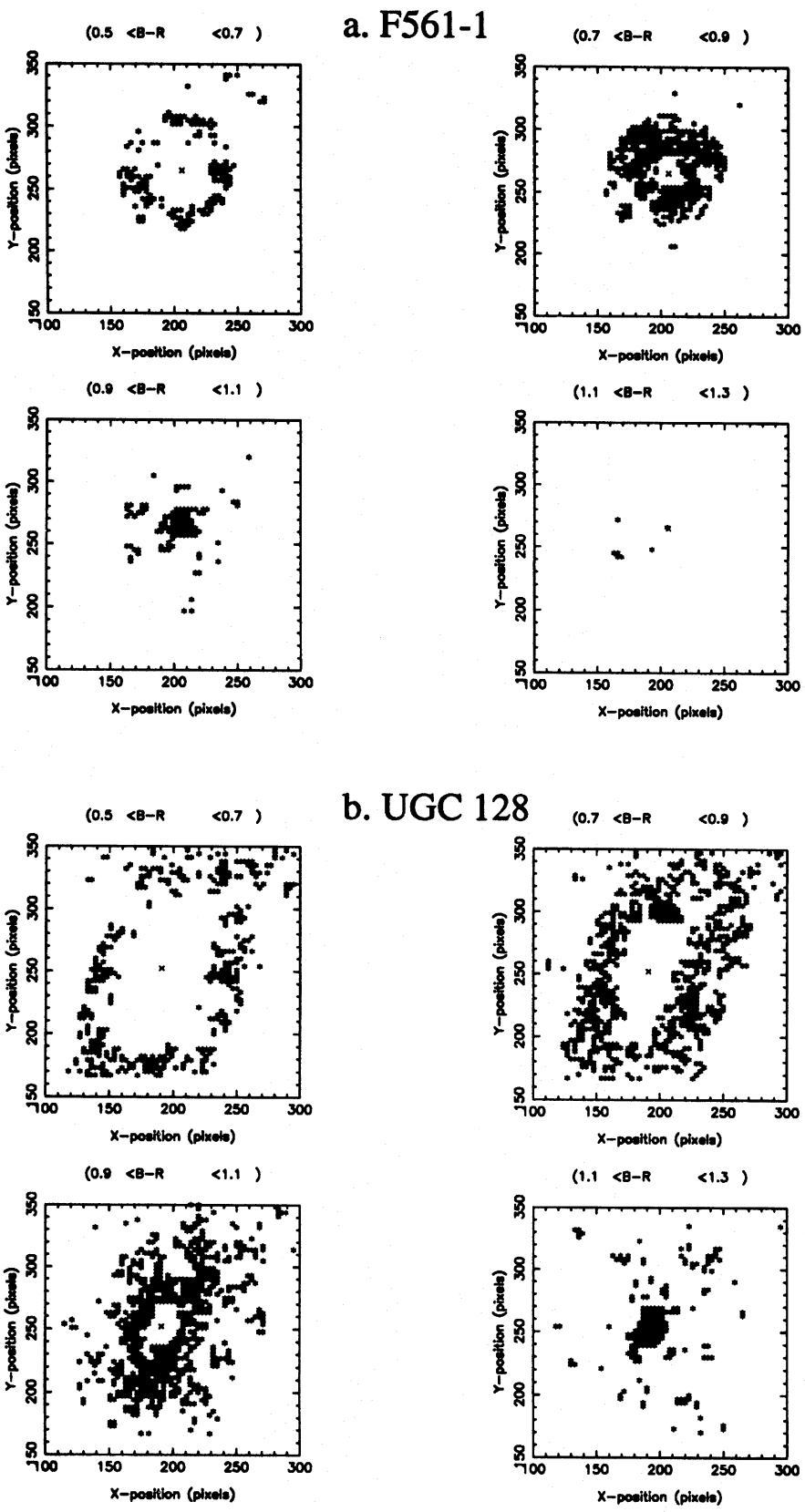

Figure 6. Two-dimensional $B - R$ colour distributions displayed as the areas of colour within each of four colour intervals. Note the blueing towards larger galactocentric radii. (a) F561-1, (b) UGC 128.

Table 4. Colours of LSB galaxies.

Name	$U-B$			$B-V$			$B-R$			$V-I$			r_{max}
	nuc	lum	area	nuc	lum	area	nuc	lum	area	nuc	lum	area	(″)
F561-1	0.04	-0.04	-0.20	0.62	0.55	0.49	0.98	0.82	0.70	0.79	0.76	0.66	22
F563-1	0.23	0.07	-0.05	0.67	0.64	0.58	1.03	0.96	0.84				16
F563-V1	0.05	-0.01	-0.05	0.55	0.59	0.59				0.71	0.71	0.69	15
F564-V3				0.57	0.57	0.56	0.88	0.87	0.80				16
F565-V2				0.52	0.51	0.49	0.83	0.82	0.81				15
F567-2	0.05	-0.05	-0.14	0.69	0.61	0.57	1.04	0.91	0.77	0.71	0.73	0.62	16
F568-1	0.21	-0.09	-0.20	0.71	0.58	0.53	1.14	0.95	0.80	0.86	0.88	0.76	24
F568-3	0.06	-0.04	-0.11	0.70	0.61	0.54	1.10	0.94	0.81	0.88	0.84	0.72	23
F568-V1	0.11	-0.16	-0.15	0.61	0.57	0.56	1.03	0.91	0.82	0.84	0.77	0.67	19
F571-5	-0.06	-0.12	-0.13	0.56	0.54	0.44	0.87	0.85	0.74				13
F571-V1				0.58	0.55	0.51	0.93	0.89	0.78				17
F574-2				0.63	0.59	0.51	0.96	0.86	0.70				22
F577-V1	-0.12	-0.19	-0.40	0.54	0.50	0.40	0.87	0.77	0.58				17
UGC 0128	0.36	0.16	0.02	0.73	0.60	0.49	1.16	0.90	0.73	0.85	0.68	0.55	48
UGC 0628	0.19	0.04	-0.07	0.75	0.61	0.53	1.17	0.98	0.86	0.97	0.89	0.78	40
UGC 1230	0.01	-0.19	-0.30	0.63	0.54	0.47	0.98	0.89	0.76	0.92	0.86	0.77	28

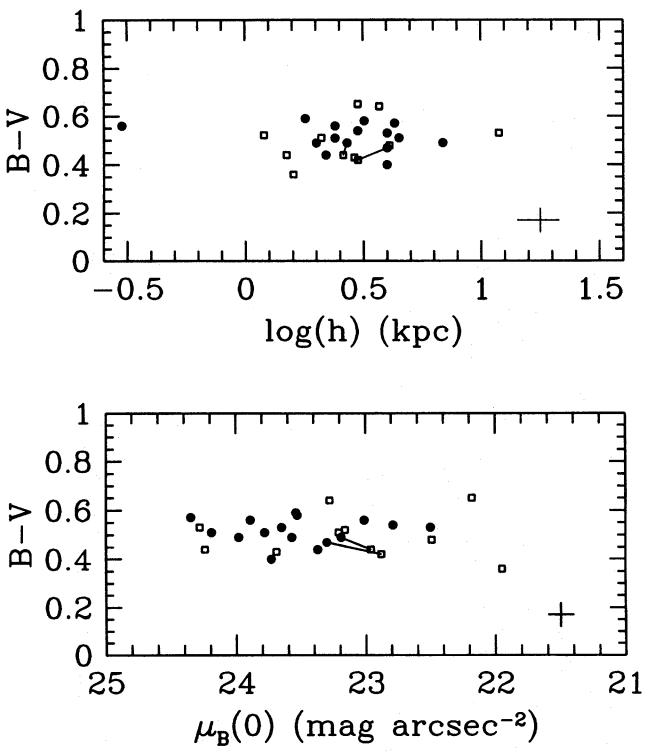

Figure 7. (a) Distribution of $B-V$ colour as a function of scale length. The black dots represent our sample, the open squares McGaugh's sample. Common galaxies are connected. The cross shows the typical errors. (b) Distribution of $B-V$ colour as a function of central surface brightness. The black dots represent our sample, the open squares McGaugh's sample. Common galaxies are connected.

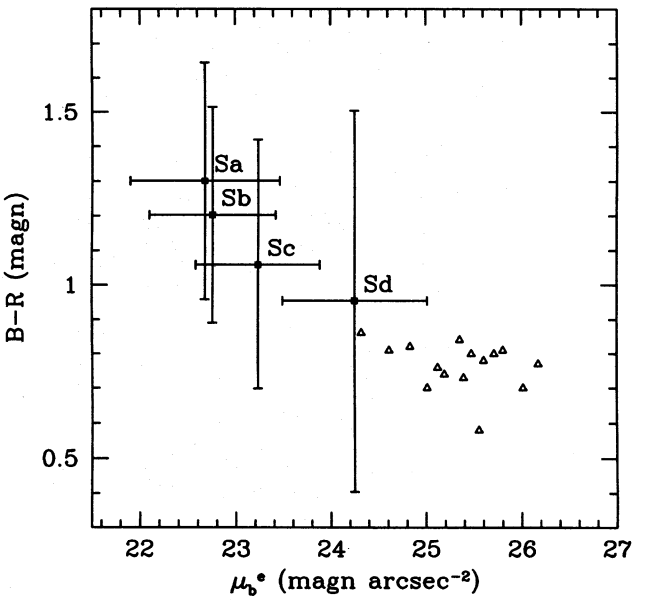

Figure 8. $B-R$ colours of HSB and LSB galaxies as a function of effective surface brightness. The triangles represent our sample of LSB galaxies. The squares and error bars represent the mean values and 1σ deviations for all Sa, Sb, Sc, and Sd galaxies in our ESO-LV sample.

Tables 3 and 4. When discussing colours, any effects that internal extinction may have are ignored.

F561-1 shows no clear spiral structure, but instead shows a ring of bright knots, which are very probably star forming regions. The ring can be seen as a bump in the radial profiles at $r \sim 15$ arcsec. It is not very apparent in the colour profiles, except perhaps for a small blueing in $V-I$ at that radius. The colour gradient is steepest for $U-B$. This fact, together with the central reddening in $V-I$ (which most likely is not a seeing effect), seems to suggest that star formation may have started in the central parts, and has now progressed to the outer parts (the ring of star forming regions) while it has declined in the centre.

F563-1 has a peculiar morphology, dominated by a very bright region to the west of the centre. This region is part of a partial ring of star forming regions. It shows no clear spiral structure, and fades out to the east of the centre, while the light cut-off is rather sharp towards the star formation regions. The star formation regions are only apparent as a bump in the U profile at $r = 10$ arcsec, and not in the colour profiles, except for the slight blueing in the $U-B$ profile. In this profile we

also find the strongest gradient of the entire sample. It can be caused by the same scenario as in F561-1: star formation has started in the centre, and has now progressed outward to the partial ring of star forming regions. Close examination of the optical image shows that optical emission can be traced out to ~ 1 arcmin from the centre. The isolated object 40 arcsec to the SW may in fact lie at the tip of a very faint spiral arm, and the entire galaxy may be surrounded by a very LSB spiral disc. The available WSRT H I imaging (de Blok, McGaugh & van der Hulst, in preparation.) supports this: the galaxy is surrounded by a very large H I disc, which is about 4 times larger than the optical size.

F563-V1 is an amorphous galaxy with no spiral structure visible. The radial profiles show it to be an almost perfect exponential disc. There are no obvious star formation complexes in this galaxy, except for one faint star formation region to the south of the centre. The gradients in this galaxy are very small, suggesting that here no progression of star formation has taken place: the disc is a homogeneous mix of different stellar populations.

F564-V3 is amorphous and diffuse. It shows no structure, apart from a general brightening towards the centre. The colour gradients per arcsecond are very small, but its surface brightness profiles show it to be not a perfectly exponential disc. The radial profiles all flatten towards the centre. It is the only galaxy in our sample where a significant flattening of the profile near the centre occurs. Its H I redshift is only 500 km s^{-1} (SBSM), placing it at a distance of ~ 6 Mpc. Assuming that this distance is correct, it is the smallest galaxy in our sample, with a scale length of only 0.3 kpc. This could mean that F564-V3 is a true dwarf galaxy.

6 DISCUSSION OF THE COLOURS

6.1 Median colours

We will discuss the colours of LSB galaxies, and compare them with evolutionary models from the literature, with the goal of tracing a possible star formation history for these objects. Where possible we will supplement our data with those of McGaugh (1992), who has used the same selection criteria for his sample as we have. A comparison of the photometry of the few galaxies that our sample and McGaugh's sample have in common shows that any systematic differences between the measurements are much smaller than the typical errors in the colours. Comparisons with independent observations of UGC 628 (Knezek 1993; de Jong & van der Kruit 1994) give differences in the measured $B-R$ colour profiles of < 0.1 mag.

In order to make comparisons with colours of other types of objects we will assume that the median area-weighted colours of our and McGaugh's samples combined are representative for the sample as a whole. The median area-weighted colours of the combined sample are $U-B=-0.13$, $B-V=0.51$, $B-R=0.78$, and $V-I=0.76$. These colours are also given in Table 5. The large difference in $V-I$ between our and McGaugh's samples is immediately apparent. For the galaxy F563-V1, which is common to both samples, there is a large difference in the colours as determined by McGaugh and us. According to McGaugh (private communication) this may be due to a defect in his V-image of this galaxy. This galaxy is therefore excluded from any discussion about McGaugh's sample. A possible explanation for the difference between our and McGaugh's $V-I$ colours is that McGaugh's sample simply contains more galaxies that are redder in $V-I$ than our sample.

Table 5. Comparison of colours.

Col (1)	Our (2)	McG (3)	Comb (4)	HSB (5)
$U-B$	−0.14	−0.12	−0.13	−0.14
$B-V$	+0.52	+0.44	+0.51	0.51
$B-R$	+0.78	–	+0.78	0.92
$V-I$	+0.69	+0.95	+0.76	0.90

(1) colour
(2) our median values
(3) McGaugh's median values
(4) combined median values
(5) colours of HSB galaxy

6.2 Comparison with HSB galaxies

Morphology shows that very late-type HSB galaxies (Sd and later) are the most likely candidates for comparison. These too have small to absent bulges, and loose, less strongly developed spiral arms. There are of course also differences, such as the number of H II regions present, and thence the amount of star formation.

We have used the RC3 (de Vaucouleurs et al. 1991), the ESO-LV (Lauberts & Valentijn 1989), and results from Huchra (1977), Byun (1992) and Han (1992) to determine the colours of typical HSB Sdm–Sm (comparison) galaxies. These colours are $U-B=-0.14$, $B-V=0.51$, $B-R=0.92$, and $V-I=0.9$ (cf. Figs 9 and 10). The scatter in $B-R$ and $V-I$ is quite large (Han 1992; ESO-LV). The value of $V-I$ is rather uncertain due to the fact that Han's corrections for extinction are larger than we expect them to be for these late-type galaxies.

Comparison with Table 5 shows that $U-B$ and $B-V$ of LSB galaxies are roughly equal to those of late-type HSB galaxies. Blue colours are generally associated with star formation, which is definitely taking place in late-type HSB galaxies. It is surprising that LSB galaxies that have no or only small traces of star formation, and which generally look much more quiescent, should have comparable colours. The presence of only small amounts of star formation is confirmed by Hα imaging (McGaugh 1992; de Blok, McGaugh & van der Hulst, in preparation). For a further discussion see Sections 6.5 and 7.

Fig. 9 shows a UBV diagram for the roughly 500 late-type galaxies (Sc and later) for which both $U-B$ and $B-V$ were available in the RC3. We have binned these galaxies per Hubble type, and have plotted the mean colours and 1σ deviations. It is clear that there is a trend of colour with Hubble type, in the sense that galaxies become bluer toward later Hubble type. It is also clear that the spread in colour for a given type is so large that we cannot use the colour of a galaxy as a good measure for its Hubble type. The stars in Fig. 9 represent the LSB galaxies from both our and McGaugh's samples. These galaxies have colours that scatter around the typical colours for Sdm and Sm galaxies.

Fig. 10 shows a BRI diagram. The mean colours and

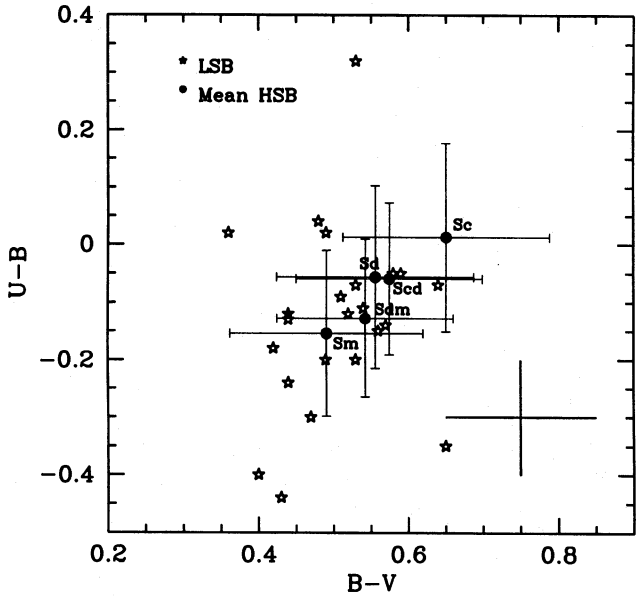

Figure 9. *UBV* diagram. The filled circles represent the mean colours for each Hubble type. The error bars denote 1σ deviations from the mean colours. The stars represent the colours of the LSB galaxies.

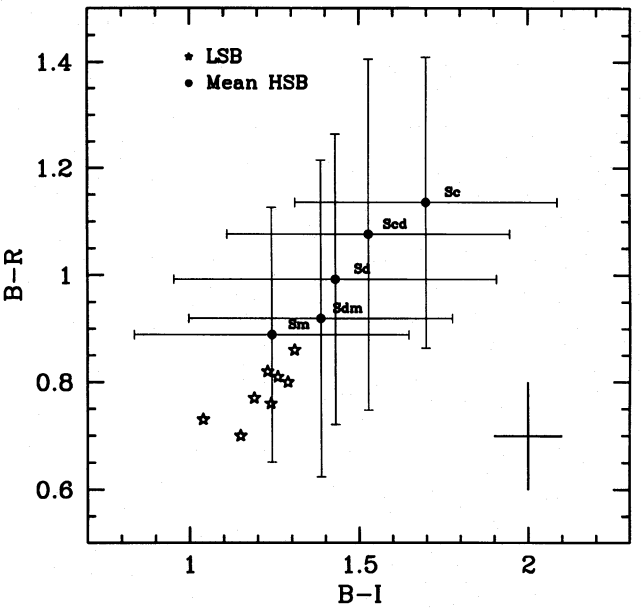

Figure 10. *BRI* diagram. The filled circles represent the mean colours for each Hubble type. The error bars denote 1σ deviations from the mean colours. The stars represent the colours of the LSB galaxies.

1σ deviations of the $\sim$ 200 late-type galaxies (Sc and later) for which both colours were available in Byun (1992) and the ESO-LV are shown, binned per Hubble type. The stars represent the LSB galaxies. Once again there is a clear trend of colour with Hubble type, and once again colour does not correspond unambiguously with Hubble type. It is clear that in these colours the LSB galaxies are consistently bluer than Sdm–Sm HSB galaxies.

6.3 Dust and extinction effects

Since LSB galaxies are bluer than HSB galaxies, one could assume that LSB galaxies are dustless HSB galaxies. To explain the colours, LSB galaxies then need on average $\sim$ 0.5 mag less extinction in the V-band than HSB galaxies, assuming that the mix of stellar populations in LSB and Sc galaxies is equal, and using the simple absorbing, overlying screen model for the extinction and reddening. LSB galaxies should then have a higher surface brightness than HSB galaxies, which is obviously not true.

However, the assumption of identical stellar populations is not likely to be true, in view of the different star formation histories, as we will discuss later. The assumption of an overlying screen is naive and too simplistic. As Disney, Davies & Phillips (1989) and Witt, Thronson & Capuano (1992) have shown, the screen model is not the most realistic model. Reddened stars will become fainter and more obscured, and thus will contribute less red light to the total colour, so that the least obscured parts of a galaxy will determine its colours. So dust may be present in different quantities in LSB and Sc galaxies, but we are unable to derive these quantities using just broad-band optical colours. In both LSB and Sc galaxies we may therefore expect global colours to be largely determined by stars that are not or only lightly obscured by dust.

Furthermore, for a correct analysis of extinction and reddening, one also has to take scattering into account. As suggested by the models described in Elmegreen (1980) and Rix & Rieke (1993), scattering is particularly important in our case where we study face-on galaxies at optical wavelengths. Photons that get scattered will have a greater chance of being scattered out of the disc perpendicularly (in the face-on direction) than in the edge-on direction (in the plane of the disc), where they have a larger chance of being absorbed. The scattered photons that reach us will effectively make the observed colours bluer again, bringing them closer to their intrinsic values.

Dust will play a role in determining colours but it is certainly not able to explain the difference in colours between LSB and Sc HSB galaxies entirely. Age and metallicity effects must also play a role.

6.4 Metallicity effects: comparison with globular clusters

McGaugh (1994) has shown that LSB galaxies have low metallicities and it is known that low metallicity gives rise to bluer colours. To get an idea of the magnitude of this effect we can look at metal-poor objects, and compare their colours with those of the LSB galaxies. We will not compare the sample with, for example, blue compact galaxies: although these objects have low metallicities, the high star formation rates they exhibit make them unsuitable for a comparison. Better comparison objects are metal-poor globular clusters.

For metal-poor globular clusters ([Fe/H] $\simeq -2.0$) one finds $U-B = 0.1$, $B-V = 0.65$, $B-R = 1.1$ and $V-I = 0.95$ (Reed 1985; Reed, Hesser & Shawl 1988; Hesser & Shawl 1985). These globular clusters are therefore generally redder than the LSB galaxies. Globular clusters in the Magellanic Clouds (Elson & Fall 1985) are also redder. These very metal-poor objects show $U-B = 0.2$ for a $B-V$ colour equal to that of the median $B-V$ colour of the sample. *Globular clusters are thus much redder than LSB galaxies.* Although part of the blue

colours could be caused by metallicity effects (e.g., by having an old metal-poor population), these effects cannot explain the colours completely. Age must certainly play a major role.

The ambiguity between age and metallicity also affects the interpretation of the measured colour gradients. The general trend towards bluer colours with increasing radius could be a reflection of lower metallicity in the outer parts or it could represent a difference in mean age between the inner and outer regions. This is not entirely unreasonable, as LSB galaxies may have long collapse times and thus star formation may proceed first in the inner, denser regions while the outer regions are still collapsing.

6.5 Age effects

The $U-B$ and $B-V$ colours, which are comparable to those of HSB galaxies, and the presence of a small number of star forming regions imply that part of the stellar content of LSB galaxies must consist of young stars. However, the lack of a *large* number of prominent star forming regions suggests that star formation should be taking place diffusely across the disc. We constructed a simple model to test the effects of star formation on the total colours. This model consists of a red population with the properties of metal-poor globular cluster stars, as described in Section 6.4. To this red population an increasing number of B-stars were added, and the effect on the total colours was calculated. This rather naive model suggests that approximately 5 to 10 per cent of the area of the disc should in some way be affected by star formation, in order to have a noticeable ($\sim$ 0.1 mag) effect on the total colours. Judging from colour maps (see e.g. Fig. 6), 5 to 10 per cent is not an unreasonable value.

The galaxies in our sample look similar to galaxies of late Hubble type and their properties are just as heterogeneous as those of HSB galaxies, with a variety in colour, surface brightness, morphology and size. Each of these galaxies is likely to have its unique star formation history, presumably different from those of HSB galaxies.

7 DISCUSSION

In this section we will not try to decipher the star formation history and evolution in detail. Rather we will describe a few possible star formations scenarios that may apply to LSB galaxies, and discuss their possible merits and shortcomings.

It is a challenge to model the evolution of these galaxies and we hope to do this at a later stage. The range of properties (gas density, metallicity, star formation rate) is so wide that many of the published galaxy evolution models only cover a small section of parameter space, and it is beyond the scope of this paper to fix that shortcoming here. Rather we will refer to published models of the star formation histories of HSB galaxies, in particular Searle, Sargent & Bagnuolo (1973), Larson & Tinsley (1978), Guiderdoni & Rocca-Volmerange (1987) and Mazzei, Xu & De Zotti (1992). We realize that the published models were mostly computed assuming solar metallicity. As the metallicity in LSB galaxies, as measured in H II regions, is about a fifth of the solar metallicity, it is likely that the metallicity of the stellar population is less than this value. We do realize this severe shortcoming, but, rather than paying too much attention to the absolute values of the colours, we will use the models as a reference to elucidate possible star formation histories.

7.1 Disc-fading scenario

This scenario would seem to be a very natural explanation for the nature of LSB galaxies: they are simply assumed to be the faded remnants of once normal disc galaxies that for some reason have ceased to form stars a few billion years ago. We can, however, use our data as presented in Fig. 7 and the simple models of Searle et al. to disprove this scenario. In the absence of star formation a galaxy will become redder and fainter with time (regardless of metallicity), as the short-lived blue stars die. From Searle et al. we can derive a reddening of 0.22 mag in $B-V$ for each magnitude fading in B. If this scenario were correct Fig. 7 should have shown at least a clear reddening with decreasing surface brightness. *LSB galaxies are not the faded remnants of normal HSB galaxies.*

7.2 Initial starburst with cutoff

An initial starburst with subsequent cutoff in star formation is equivalent to the disc-fading scenario, and is therefore not likely to explain the observed colours. Indeed, for a model that has an initial starburst with cutoff after 10^7 years, Larson & Tinsley (1978) find colours that are too red to fit our measured colours.

7.3 Exponentially declining star formation rate

The exponentially declining star formation rate (SFR) has frequently been used as the 'standard' star formation history for spiral galaxies. This scenario can result in the low present SFR that we measure in LSB galaxies.

The colours at the blue end of the spectrum, $U-B$ and $B-V$, are very similar to those of HSB galaxies, as noted in previous sections. This is understandable, as these colours are sensitive to recent star formation, and this recent star formation is, albeit in different quantities, present in both HSB and LSB galaxies. So to see whether the exponentially declining SFR is valid we have to look at the presence or absence of a large old, red population, as the exponential nature of this star formation history implies that the amount of stars formed in the past was much greater, and consequently any galaxy that has undergone an exponential star formation history must have a large population of old stars. The bulk of these stars will have their peak optical emission at the red end of the spectrum, i.e. we will mainly detect them in the R- and I-bands, and the colours will then be equal to those of late-type HSB galaxies that have had much star formation in the past. The $B-R$ and $V-I$ colours of LSB galaxies are significantly bluer than those of HSB galaxies, which suggests a relative lack of this old population.

$V-I$ furthermore is an indicator of the position and degree of development of the giant branch in the HR-diagram (Bothun et al. 1984) and therefore metallicity dependent, as the position of the giant branch in the HR-diagram changes with metallicity. The values found for $V-I$ thus also suggest low metallicity and no early enrichment of the interstellar medium, once again suggesting a lack of major star formation in the past. Observations in the near-infrared (in J, H and K: see

Bothun & Gregg 1990) combined with measurements of the metallicities are needed to prove this, as an old population will manifest itself clearly in the near-infrared.

LSB galaxies have not undergone an exponentially declining star formation history.

7.4 Constant star formation rate

A constant SFR is also excluded for the same reasons as above: it can reproduce the measured $U-B$ and $B-V$ colours (Larson & Tinsley 1978), but only because there is some recent star formation present in LSB galaxies, as our Hα imaging shows (see also McGaugh 1992). A constant SFR also implies that by now a large old population should have announced its presence in the $B-R$ and $V-I$ colours. A further clue can be found in the models of Mazzei et al. (1992). These models take some chemical evolution into account, and the poorly known evolution of stars in their giant phases. One finds that the $U-B$ and $B-V$ colours can only be modelled using an age of 10 Gyr, while the $B-R$ and $V-I$ can only be modelled using an age between 2 and 5 Gyr. Although the absolute values of the colours will probably not be right due to the differing metallicities, the trend in age suggests we need an underdeveloped (with respect to the HSB galaxy case) old population to explain the differences between the red and the blue colours [cf. the constant SFR models of Guiderdoni & Rocca-Volmerange (1987): their 9.5-Gyr models give a better approximation to the colours than their 15.5-Gyr models].

7.5 Sporadic star formation rate

The lack of clear signs of an old population, combined with the fact that we still find evidence for young stars in LSB galaxies, suggests the following scenario for the star formation history of LSB galaxies. As the current metallicity is low, it is improbable that there has been a large amount of star formation in the past, be it burst-like or not. The blue $U-B$ and $B-V$ suggest that some high-mass stars are present at the moment. We can reach this stage by including small surges in the SFR, either superimposed on a very low constant SFR, or not. Where this temporary increase occurs is largely determined by the critical density for star formation in H I [see discussion by van der Hulst et al. (1993)].

Salzer et al. (1991) show that the younger a blue population is, the smaller the ratio of blue stars to red stars needs to be in order to produce blue colours. So, if indeed a small increase in the SFR leads to star formation taking place at this moment, then one only needs a small fraction of the total number of stars to be young stars to make the colours bluer. For a standard IMF, this cannot happen too often without increasing the old population, and turning the LSB disc into a HSB disc.

7.6 Summary

We can summarize the discussion as follows. The star formation scenarios suggest that the colours can be explained by assuming a less developed old population, and a more luminosity-dominant blue population. The LSB galaxies had a low (sporadic) SFR in the past, so that fewer stars were formed. Recent star formation made $U-B$ and $B-V$ bluer with respect to $B-R$ and $V-I$. The low metallicities in these galaxies will furthermore make the colours still bluer. Star formation has commenced relatively recently and an old population has not yet had time to develop. But a LSB disc can contain only a limited amount of young stars without becoming a HSB disc.

We can speculate that the LSB galaxies in our sample are ones that are at the moment going through a phase of slightly enhanced star formation. One of the problems created by assuming that this extra star formation causes the LSB galaxies to be as blue as they are is that there must then necessarily also be *red* LSB galaxies that are quiescent and not undergoing a burst. A possible reason why these galaxies are not in our sample is that the LSB galaxy catalogues by SBSM were composed after visual inspection of the *blue* POSS-2 plates. Red LSB galaxies may therefore have been missed which would serve to increase the overall space density of LSB galaxies.

An alternative reason may be that red LSB galaxies simply do not exist. In that case the present state of the LSB galaxies in our sample is typical for all LSB galaxies. But then one needs to explain why these galaxies all have recently begun to experience a period of enhanced star formation. That is to say, why, after a Hubble time, do we not find examples of red, faded discs, since surely in the future the Universe will be filled with them?

8 CONCLUSIONS

LSB galaxies have scale lengths comparable to those of late-type HSB galaxies. They do have bluer discs than HSB galaxies. The blue colours cannot be entirely explained by metallicity effects as judged from comparison with metal-poor globular clusters. Comparison with evolution models shows that part of the blue colours can be ascribed to age effects for very low star formation rate scenarios.

These scenarios can be described by low, or absent, global star formation rates, with slight increases at present or in the relatively recent past. This leads to a luminosity-dominant young population, with presumably a small, underdeveloped (with respect to HSB galaxies) old population.

It may be that the LSB galaxies we observe are going through a phase of more active star formation, as is suggested by the partial star forming rings observed in a few galaxies. The star formation is local and sporadic, as the colours do not support starbursts or vigorous star formation hypotheses. We may be seeing only galaxies that are in a more active phase, while quiescent, inactive and much redder LSB galaxies may still escape detection.

For a better determination of the star formation history of LSB galaxies we need additional information from near-infrared wavelengths and chemical abundance information to unravel age and metallicity effects.

ACKNOWLEDGMENTS

We would like to thank Stacy McGaugh and Rob Swaters for many discussions and constructive comments, and Reynier Peletier and Roelof de Jong for reading the final versions of

this paper. We thank Jon Davies for his valuable comments on the submitted version.

The Isaac Newton Telescope is operated by the Royal Greenwich Observatory at the Observatorio del Roque de los Muchachos of the Instituto de Astrofísica de Canarias with financial support from the PPARC (UK) and NWO (NL).

REFERENCES

Allen C.W., 1973, Astrophysical Quantities, 3rd edn. Athlone Press, London, pp. 263-265
Allen R.J., Shu F.H., 1979, ApJ, 227, 67
Bessell M.S., 1979, PASP, 91, 589
Bosma A., Freeman K.C., 1993, AJ, 106, 1394
Bothun G.D., 1986, AJ, 91, 507
Bothun G.D., Gregg M., 1990, ApJ, 350, 73
Bothun G.D., Romanishin W., Strom K.M., Strom S.F., 1984, AJ, 89, 1300
Bothun G.D., Schombert J.M., Impey C.D., Sprayberry D., McGaugh S.S., 1993, AJ, 106, 530
Burstein D., Heiles C., 1982, AJ, 87, 1165
Byun, Y.-I., 1992, Ph.D. Thesis, The Australian National University
Davies J.I., 1990, MNRAS, 244, 8
de Jong R.S., van der Kruit P.C., 1994, A&AS, 106, 451
de Vaucouleurs G., 1959, in Flügge S., ed., Handbuch der Physik, Vol. 53, Astrophysics IV: Stellar Systems. Springer-Verlag, Berlin
de Vaucouleurs A., de Vaucouleurs G., Buta R.J., Corwin H.G., Jr, Fouqué P., Paturel G., 1991, Third Reference Catalogue of Bright Galaxies (RC3). Springer-Verlag, New York
Disney M.J., 1976, Nat, 263, 573
Disney M.J., Phillipps S., 1983, MNRAS, 205, 1253
Disney M.J., Davies J., Phillipps S., 1989, MNRAS, 239, 939
Elmegreen D.M., 1980, ApJS, 43, 37
Elson R.A.W., Fall S.M., 1985, ApJ, 299, 211
Freeman K.C., 1970, ApJ, 160, 811
Giovanelli R., Haynes M.P., Salzer J.J., Wegner G., Da Costa L.N., Freudling W., 1994, AJ, 107, 2036
Grosbøl P.J., 1985, A&AS, 60, 26
Guiderdoni B., Rocca-Volmerange B., 1987, A&A, 186, 1
Han M., 1992, ApJS, 81, 35
Hesser J.E., Shawl S.J., 1985, PASP, 97, 465
Holmberg E., 1958, Medd. Lund. Obs. Series II, No. 136
Huchra J.P., 1977, ApJS, 35, 171
Huizinga J.E., 1994, Ph.D. Thesis, Univ. of Groningen
Impey C., Bothun G.D., 1989, ApJ, 341, 89
Kennicutt R.C., 1989, ApJ, 344, 685
Knezek P.M., 1993, Ph.D. Thesis, Univ. of Massachusetts
Landolt A.U., 1983, AJ, 88, 439
Larson R.B., Tinsley B.M., 1978, ApJ, 219, 46
Lauberts A., Valentijn E.A., 1989, The Surface Photometry Catalogue of the ESO-Uppsala Galaxies (ESO-LV). European Southern Observatory
Mazzei P., Xu C., De Zotti G., 1992, A&A, 256, 45
McGaugh S.S., 1992, Ph.D. Thesis, Univ. of Michigan
McGaugh S.S., 1994, ApJ, 426, 135
McGaugh S.S., Bothun G.D., 1994, AJ, 107, 530
Nilson P., 1973, Uppsala General Catalog of Galaxies, Ann. Uppsala Astron. Obs., 6
Peletier R.F., Willner S.P., 1993, ApJ, 418, 626
Reed B.C., 1985, PASP, 97, 120
Reed B.C., Hesser J.E., Shawl S.J., 1988, PASP, 100, 545
Rix H-W., Rieke M.J., 1993, ApJ, 418, 123
Salzer J.J., Alighieri S.D.S., Matteucci F., Giovanelli R., Haynes M.P., 1991, AJ, 101, 1258
Schombert J.M., Bothun G.D., 1988, AJ, 95, 1389 (SBSM)
Schombert J.M., Bothun G.D., Impey C.D., Mundy L.G., 1990, AJ, 100, 1523
Schombert J.M., Bothun G.D., Schneider S.E., McGaugh S.S., 1992, AJ, 103, 1107 (SBSM)
Searle L., Sargent W.L.W., Bagnuolo W.G., 1973, ApJ, 179, 427
Thuan T., Gott R., Schneider S., 1987, ApJ, 315, L93
Valentijn E.A., 1990, Nat, 346, 153
van der Hulst J.M., Skillman E.D., Smith T.R., Bothun G.D., McGaugh S.S., de Blok W.J.G., 1993, AJ, 106, 548
van der Kruit P.C., 1987, A&A, 173, 59
Witt A.N., Thronson H.A., Jr, Capuano J.M., Jr, 1992, ApJ, 393, 611

This paper has been produced using the Royal Astronomical Society/Blackwell Science LaTeX style file.